Carbonate and elemental accumulation rates in arid soils of mid-to-late Pleistocene outwash terraces, southeastern Wind River Range, Wyoming, USA

Dahms, Dennis ; Egli, Markus

Abstract: An important result of the past few decades of soil–geomorphic research is the awareness of the major role of dust and related carbonate precipitates in arid soils. The temporal evolution of soils developed on outwash terraces is still a matter of debate particularly regarding the type of evolution: progressive evolution and constant rates vs complex and/or interval-accumulation rates (progressive or regressive evolution possible). Soils on a chronosequence of outwash terraces just outside and downstream of canyon mouths of the Wind River Range (USA) were analysed for carbonate accumulation, organic carbon and poorly-crystalline pedogenetic oxyhydroxides stocks and pathways of chemical weathering. The soils and their carbonate stocks in the fine earth fraction (< 2 mm) can be used as a relative dating tool and appear to correlate with regional glacial chronostratigraphy [Pinedale (c. 20 ky), Bull Lake (with two different units around 160 and 260 ky) and Sacagawea Ridge (c. 660 ky)]. Carbonate stocks of soils on these terraces increase with increasing soil age, but at generally decreasing rates. A quasi-steady state situation, however, was not reached before 1 My. The time-split approach showed that CaCO3 accumulation rates were the highest during marine isotope (MIS) cold stages (2.13 g CaCO3/m2/y), presumably due to a sparse vegetation cover during MIS2 (Pinedale) and 8 (lower Bull lake). Compared to organic carbon (c. 8–10 kg Corg/m2), the inorganic carbon stocks of the fine earth fraction were much higher (c. 60 kg Cinorg/m2). Although the dominant pedogenic process here appears to be carbonate accumulation, chemical weathering and elemental leaching also are significant. Weathering data were obtained using immobile elements and rare earth elements (REE) as tracers. Chemical weathering and related leaching were particularly notable for Na originating from plagioclase. In addition, pedogenetic Al and Mn oxyhydroxides accumulate (220 and 32 g/m2, respectively, after 660 ky). These form at relatively low rates, however, when compared to moister and cooler conditions at higher altitudes in the Wind River Range. Due to the dry climate under which the terrace soils formed (annual precipitation 32 cm/yr− 1), weakly crystalline and amorphous Fe-oxyhydroxide is rapidly transformed into crystalline forms (hematite) over time. Consequently, the stocks of weakly crystalline and amorphous Fe-oxyhydroxide was significantly lower in the 660 ky soils (50 g/m2) than in the Holocene soils (1000 g/m2). The development of soils on Quaternary outwash terraces in this region is controlled through the rates of aeolian influx over time as modified by glacial/interglacial climate variations rather than by moisture availability. Consequently, carbonate accumulation rates in these soils are 'influx limited' rather than 'moisture limited'.

DOI: https://doi.org/10.1016/j.chemgeo.2015.12.006

Originally published at:
Dahms, Dennis; Egli, Markus (2016). Carbonate and elemental accumulation rates in arid soils of mid-to-late Pleistocene outwash terraces, southeastern Wind River Range, Wyoming, USA. Chemical Geology, 446:147-162.
DOI: https://doi.org/10.1016/j.chemgeo.2015.12.006

Carbonate and elemental accumulation rates in arid soils of mid-to-late Pleistocene outwash terraces, southeastern Wind River Range, Wyoming, USA

Dennis Dahms[1], Markus Egli[2]*

[1]Department of Geography, University of Northern Iowa, Cedar Falls, USA

[2]Department of Geography, University of Zurich, CH-8057 Zurich, Switzerland

*Corresponding author. Tel.: +41 44 635 51 14; fax: +41 44 6356848.

E-mail address: markus.egli@geo.uzh.ch (M. Egli).

Abstract

An important result of the past few decades of soil–geomorphic research is the awareness of the major role of dust and related carbonate precipitates in arid soils. The temporal evolution of soils developed on outwash terraces is still a matter of debate particularly regarding the type of evolution: progressive evolution and constant rates vs complex and/or interval-accumulation rates (progressive or regressive evolution possible). Soils on a chronosequence of outwash terraces just outside and downstream of canyon mouths of the Wind River Range (USA) were analysed for carbonate accumulation, organic carbon and poorly-crystalline pedogenetic oxyhydroxides stocks and pathways of chemical weathering. The soils and their carbonate stocks in the fine earth fraction (< 2 mm) can be used as a relative dating tool and appear to correlate with regional glacial chronostratigraphy [Pinedale (c. 20 ky), Bull Lake (with two different units around 160 and 260 ky) and Sacagawea Ridge (c. 660 ky)]. Carbonate stocks of soils on these terraces increase with

increasing soil age, but at generally decreasing rates. A quasi-steady state situation, however, was not reached before 1 My. The time-split approach showed that $CaCO_3$ accumulation rates were the highest during marine isotope (MIS) cold stages (2.13 g $CaCO_3/m^2/y$), presumably due to a sparse vegetation cover during MIS2 (Pinedale) and 8 (lower Bull lake). Compared to organic carbon (c. 8 – 10 kg C_{org}/m^2), the inorganic carbon stocks of the fine earth fraction were much higher (c. 60 kg C_{inorg}/m^2). Although the dominant pedogenic process here appears to be carbonate accumulation, chemical weathering and elemental leaching also are significant. Weathering data were obtained using immobile elements and rare earth elements (REE) as tracers. Chemical weathering and related leaching were particularly notable for Na originating from plagioclase. In addition, pedogenetic Al and Mn oxyhydroxides accumulate (220 and 32 g/m^2, respectively, after 660 ky). These form at relatively low rates, however, when compared to moister and cooler conditions at higher altitudes in the Wind River Range. Due to the dry climate under which the terrace soils formed (annual precipitation 32 cm/yr^{-1}), weakly crystalline and amorphous Fe-oxyhydroxide is rapidly transformed into crystalline forms (hematite) over time. Consequently, the stocks of weakly crystalline and amorphous Fe-oxyhydroxide was significantly lower in the ~660 ky soils (50 g/m^2) than in the Holocene soils (1000 g/m^2).

The development of soils on Quaternary outwash terraces in this region are controlled through the rates of aeolian influx over time as modified by glacial/interglacial climate variations rather than by moisture availability. Consequently, carbonate accumulation rates in these soils are ‘influx limited’ rather than ‘moisture limited’.

Keywords: Chronosequence, arid soils, carbonate accumulation, weathering, Wind River Range

1. Introduction

Pleistocene climate cycles have driven multiple glacial-interglacial episodes in most middle-to-high latitude mountain regions of the world. In North America, the U.S. Rocky Mountains consist of numerous mountain ranges that contain records of multiple glacial episodes (e.g., Richmond 1986; Dahms 2004a). The Greater Yellowstone Ecosystem occupies a central role in our conception of Pleistocene glacial history since it has the type localities for the entire Pleistocene glacial succession identified in the U.S. Rocky mountains (see Richmond 1986; Dahms 2004a; Pierce 2004). The Wind River Range (WRR) occupies the southern-most extent of the Yellowstone Ecosystem and was the locus of most early research into the Pleistocene glacial succession of the region (Blackwelder 1915; Richmond 1948, 1964, 1986; Mears, 1974). Most alpine valleys here were occupied by glaciers multiple times (Blackwelder 1915; Richmond 1973; Dahms 2004b). Morphostratigraphic evidence shows a minimum of four major glacial advances occurred here over the past ~1 My (Richmond, 1987; Hall and Shroba, 1995; Hall and Jaworowski, 1999; Dahms, 2004b).

An important result of the past few decades of soil–geomorphic research is the awareness of the major role of dust in arid (desert) and semi-arid regions of the world (e.g. Sauer et al., 2007; Muhs 2013, Muhs et al. 2014). In the southwestern U.S. the influx of calcareous dust is central to the genesis of calcic and petrocalcic horizons in desert soils (Gile et al., 1981; Reheis et al., 1992; McFadden, 2013). Those soils that develop beneath desert pavements of the arid southwestern U.S. form in parent materials increasingly composed of entrapped dust that is subsequently translocated below the pavement to 'build' the soil from above (McFadden, 2013).

Soils developed on Quaternary deposits of semi-arid (non-'desert') regions of the U.S. also exhibit significant contents of aeolian material (Colman and Pierce, 1986; Sorenson 1987; Reheis, 1988, 1990; Muhs et al., 1990; Reheis, 1990; Dahms 1993; Dahms and Rawlins 1996) as do soils of alpine regions of the western U.S. (Marchand 1970; Birkeland 1973; Williams 1973; Thorn and

74 Darmody 1980; Boulding and Boulding 1981; Shroba and Birkeland 1983; Swanson 1985;
75 Birkeland et al. 1987; Litaor, 1987, 1988; Dixon, 1992; Muhs and Benedict, 2006).
76 We previously described soils developed on moraine chronosequences of the WRR and found clear
77 aeolian signals in their particle size distributions, heavy mineral fractions and geochemical
78 signatures (Dahms 1993, 2004b; Dahms and Rawlins 1996; Applegarth and Dahms 2001, 2004;
79 Dahms et al., 2012). Few studies exist in this region, however, that describe soil chronosequences
80 from the outwash terraces downstream of the moraine units. Soil characteristics are reported from
81 terrace chronosequences of the Wind River in the central Wind River Basin upstream from the
82 confluence of the Wind and Popo Agie rivers (Nettleton and Chadwick, 1991) and soils on the
83 terraces of Rock Creek, a tributary of the Bighorn River are reported from the northern Big Horn
84 Basin (Reheis, 1987, 1988, 1990). No previous data exists for tributary streams emanating from the
85 glaciated valleys of the eastern slope of the Wind River Range.
86 In this study we report a suite of newly-developed chemical weathering data for a chronosequence
87 of soils on terraces of the three forks of the Popo Agie River near Lander, Wyoming. These data
88 will contribute further to the development of soil chronosequences and will function as relative-age
89 tools for correlating Pleistocene terraces in this region to their corresponding moraine units (Dahms,
90 2010). In order to further develop evidence relating to the contribution of aeolian materials, and
91 especially carbonate, to soil development over time on Quaternary alluvium in the Wind River-
92 Yellowstone region (Hall, 1999), we describe a chronofunction for carbonate accumulation and try
93 to derive, where possible, the corresponding interval accumulation rates (progressive or regressive
94 evolution possible). Few data sets exist for long-term trends in production and accumulation of
95 oxyhydroxides of Fe and Al in arid-lands soils such as these. Our results suggest that as weathering
96 and pedogenesis proceeds over time, secondary mineral phases of Fe and Al form that initially have
97 poorly/weakly crystalline characteristics, but develop strongly crystalline forms with time.
98 Furthermore, disagreement exists as to whether such soils develop linearly and progressively or

99 if/when a quasi-steady state situation is ever reached (cf. Reheis, 1990; Reheis et al., 1992; Landi et
100 al., 2003).
101
102
103 **2. Study Region**
104 The study region is on the southeastern end of the Wind River Range, near Lander, Wyoming (Fig.
105 1). The drainages of the Popo Agie basin flow from the southernmost glaciated region of the range.
106 The Popo Agie basin drains most of the alpine region of the southeastern Wind River Range (Fig.
107 1). All three tributaries (the North, Middle, and Little Popo Agie) were occupied by Pleistocene
108 valley glaciers, resulting in the formation of a four-fold sequence of outwash terraces along each of
109 these streams as presumed floodplain aggradation during each glacial maximum gave way to stream
110 incision during the post-glacial period(s) (Vandenberghe, 2015).
111 The North Fork of the Popo Agie drains the Cirque of the Towers; the Middle Fork of the Popo
112 Agie drains Deep Lakes, Ice Lakes, Stough Lakes, and Leg Lake basins; the Little Popo Agie drains
113 the Silas and Christina Lake cirques (Fig. 1). The presence of well-preserved moraines near the
114 mouths of their canyons indicates that the valleys of all three of the rivers were occupied by glaciers
115 at least four times during the last ~1 Ma (Dahms 2004b and unpublished map data). We chose to
116 study the Popo Agie basin because the outwash terraces (Fig. 2) are well-expressed and appear
117 generally to correspond to previously-mapped terrace units along the Wind River (Chadwick et al.,
118 1997; Hancock et al., 1999; Dahms 2010) to which the Popo Agie river grades (Fig. 1) and on
119 which soils are previously described (Nettleton and Chadwick, 1991).
120 The Pleistocene terraces we studied are all within 5 miles of the mouth of their canyons (Fig. 2). All
121 terraces but the Holocene unit (PB-13-1) are strath terraces (e.g., Bierman and Montgmery, 2014)
122 formed as the rivers cut into the sedimentary units that crop out along the southeastern flank of the
123 WRR (Fig. 2). Terraces along the Little Popo Agie River have slightly different sedimentary and

soil parent material characteristics. These are inset into carbonate-bearing 'Redbeds' of the Red Peak/Chugwater formations (Picard, 1993), so the coarse gravels of granitic and sedimentary origin from the interior massif and inner canyon grade upward to clays, silts, and fine sand derived exclusively from the redbeds (Fig 2d,e). Consequently, the parent materials of the soils on the Little Popo Agie River terraces contain varying amounts of $CaCO_3$ (see Table 1). The soil parent materials of the North and Middle Forks of the Popo Agie River are derived primarily from non-calcareous granitic alluvium (Table 1) from the interior of the Wind River Range and from outwash derived from upstream moraines (see Dahms, 2004a,b). The only terrace that contains fines derived from redbeds in our present sequences along the North and Middle forks is the terrace represented by sample GalPD (Fig. 2).

The climate of the lower slopes and piedmont of the eastern Wind River Range near Lander is classified as semi-arid (Köppen *Bsk*) with a mean annual maximum temperature of 14°C, a mean annual minimum temperature of 0°C and a MAT of 7°C (2015 US Climate Data). Mean annual precipitation at Lander is 320 mm. All terrace sites of the study area are grassland/sagebrush steppe, with riparian areas adjacent to the streams. The terrace soils (Fig. 3) are classified in the U.S. taxonomic system as Aridisols and Inceptisols (Soil Survey Staff, 2014). The more well-developed soils can be classilfied as Petrocryids/Calcicryids and the less-developed soils as Haplocryids.

Age control for terraces in this study is provided by geomorphologic mapping, including relative-age relationships (Dahms unpublished maps), correlations with ^{10}Be and ^{26}Al boulder-surface exposure ages from local moraine units of the Wind River Range (Gosse et al., 2003; Fabel et al., 2004; Dahms, 2004b; Dahms and Egli, unpublished data) and correspondence to terraces and soils of the Wind River (Hancock et al., 1999; Hall and Jaworowski, 1999; Jaworowski, 1992; Nettleton and Chadwick, 1991). We also take into account the ages suggested for terraces along Rock Creek, a tributary to the Bighorn River in the northern Bighorn Basin (Reheis, 1987). The Bighorn River is the name assigned to the Wind River as it flows through the Bighorn Basin downstream of Wind

River Canyon (Fig. 1). For purposes of this study, we assign the following tentative ages to the Popo Agie terraces and soils: Holocene (5 ky ± 3 ky; profile PB-13-1), Pinedale (20 ky ± 4 ky; profiles GalPD and RCT-2), 'lower' Bull Lake (160 ky ± 30 ky; profiles LWS, RCT-3, GR-13-1), 'upper' Bull Lake (260 ky ± 30 ky; profiles RCT-4, SB, GR-2) and Sacagawea Ridge (660 ky ± 80 ky; profiles RCT-5, PB-13-2). We associate these ages, respectively, with Marine Isotope Stages 1 – 2 – 6 – 8 and 16. An additional numeric age to which we can correlate locally comes from a Lava Creek ash deposit (c. 640 ky) reported by Jaworowski (1992) from the gravels of the highest 'airport' terrace at Lander, from which no soil is reported here (Fig. 2B).

3. Materials and methods

3.1. Sampling strategy

Soils were sampled and described from hand-dug pits on flat summit-shoulder positions using standard methods and horizon nomenclature (Fig. 3; Birkeland et al., 1991; Soil Survey Division Staff 1993). To obtain a detailed and long-term chronosequence, we sampled 11 terraces having an age of a few thousands of years (Holocene) to more than 600 ky. Profiles were dug to the C horizon when possible. About 2 kg of soil material per horizon were taken for the analyses (Hitz et al., 2002).

3.1. Physical analyses

Laboratory analyses of soil physical characteristics used standard techniques modified from Jackson (1969), Klute (1986) and Singer and Janitsky (1986). Particle size-distribution of the <2 mm fraction was determined as weight percent (USDA scale) using the sieve-and-pipette method with prior oxidation of organic matter by 30% H_2O_2, removal of pedogenic carbonate via 0.5N HCL on heat (~80^{o}C) and is reported as weight percent (USDA grain-size scale). The bulk density (fine

174 earth and soil skeleton) was estimated from corresponding horizons of previously-reported soils for
175 which BD was determined from gravel-free paraffin-coated peds using an estimated gravel density
176 of 2.6g/cm^{-3} (Dahms, 2002, 2004).
177
178 *3.2. Chemical analyses*
179 Oven-dried samples (70 ºC) were sieved to < 2 mm (fine earth) and homogenised with a sample
180 separator (Rentsch PT 1000). Soil-pH (0.01 M $CaCl_2$) was determined using a soil:solution ratio of
181 1:2.5. Carbonates were determined by using two different techniques. One consisted in the
182 dissolution of carbonates using HCl. The results were then compared with total Ca and Mg
183 concentrations obtained from XRF measurements. We performed an iterative speciation calculation
184 with the XRF data based on elemental contents and presented as oxides or carbonates (and fitted to
185 100% as total sum) to determine CaO, $CaCO_3$, MgO and $MgCO_3$ species. Organic C and N contents
186 (determined in duplicate) of the soil were measured at 550 °C using a C/H/N analyser (Leco). The
187 standard reference material is EDTA (Säntis Analytical, article no SA502092) having C = 41.09%,
188 H = 5.52%, N = 9.58%, O = 43.8% (measured values were C: 41.11±0.08%; H: 5.53±0.08%; N:
189 9.57±0.08%, O: 43.79±0.08).
190 Fe, Al and Mn concentrations were determined (in duplicate) after treatment with NH_4-oxalate
191 (buffered at pH 3; McKeague et al., 1971). The extracts were centrifuged for 8 minutes at 4000 rpm
192 and filtered (mesh size 0.45 µm, S&S, filter type 030/20). Element concentrations were measured
193 using atomic absorption spectroscopy (AAnalyst 700, Perkin Elmer). The blank values measured
194 (Fe: -0.23 ±0.06 mg/l; Al: -0.04 ± 0.8 mg/l; Mn: -0.005 ±0.004 mg/l) were considered for the
195 elemental concentrations. Element concentrations were furthermore controlled using standard
196 addition (recovery ≥ 95%). The oxalate treatment extracts both the weakly- and poorly crystalline
197 phases and some of the organic phases, but normally does not dissolve the strong humus-metal
198 complexes (Mizota and van Reeuwijk, 1989). A portion of each oxalate extraction was analysed for

199 rare earth elements (REE) with an Agilent 8800 Triple Quadrupole (QQQ-ICP-MS). Prior to ICP-
200 MS analyses, standard solutions were prepared from SPEX multi-element plasma standard (Spex
201 CertiPrep, NJ, USA) at 0, 10, 50, 100, 500 and 1000 ppb to derive calibration curves. Concentration
202 of REEs were measured from standard solutions, reference material (CCRMP, REE-1), blank and
203 soil samples. Repeated measurements of the standards showed that the precision error was less than
204 8%.
205 The total elemental content was determined by X-ray fluorescence. Soil material was milled to < 63
206 µm in a tungsten carbide disc swing mill (Retsch® RS1, Germany). Powder samples (in duplicates)
207 of approximately 5 g material were analysed with an energy dispersive He-flushed X-ray
208 fluorescence spectrometer (ED-XRF, SPECTRO X-LAB 2000, SPECTRO Analytical Instruments,
209 Germany). The quality of the analyses was checked using a soil reference material (Reference Soil
210 Sample CCRMP SO-4, Canada Centre for Mineral and Energy Technology) with certified total
211 element concentrations. Element recovery and detection limits are given in Appendix A.
212
213 *3.3. Soil mineralogy*
214 We used XRD (X-ray diffraction) and DRIFT (Diffuse Reflectance Infrared Fourier Transform
215 spectroscopy) analyses to qualitatively describe the soils' mineralogical properties. An overview of
216 the mineral content in the fine silt and clay fraction (< 32 µm) was obtained by scanning randomly
217 oriented samples from 2 to 80°2θ with steps of 0.02°2θ at 10 s intervals using a Bruker AXS D8
218 Advance (CuKα).
219 DRIFT-spectra (Bruker, Tensor 27) were recorded from 4000 to 250 cm^{-1} using a powder
220 containing 30 mg of sample (10% of the total weight) and 270 mg KBr (90% of the total weight).
221 Prior to measurement, the samples were again oven-dried at 60° C. The FT-IR spectra were
222 interpreted using the OPUS 6.5 software.
223

3.4. Weathering indices

Weathering characterization is based on the calculation of elemental losses from soil or sediment profiles. Relative elemental losses can be calculated using the open-system mass transport function $\tau_{j,w}$ (Chadwick et al., 1990):

$$\tau_{j,w} = \left(\frac{C_{j,w} \cdot C_{i,p}}{C_{i,w} \cdot C_{j,p}} \right) - 1 \quad (1)$$

where i denotes the immobile element (Ti), $C_{j,p}$ (g/kg) is the concentration of element j in the unweathered parent material and $C_{j,w}$ is the concentration of element j in the weathered product (g/kg).

Mourier et al. (2008) showed that rare earth element (REE) geochemistry of lacustrine sediments and soils is useful for reconstructing the history of landscape evolution. Normalised REE patterns may provide a tracer of the degree of weathering of materials. In contrast to Mourier et al. (2008), the REE concentrations were not normalised to a chondritic reference standard (Sun and McDonough, 1989) but to the parent material of the soils to better facilitate the interpretation of weathering behaviour (cf. Scarciglia et al., 2009, 2011) between sites. Normalisation against a common reference helps to identify subtle fractionations and anomalies in elemental abundances (Mourier et al., 2008). Only a portion of the REEs could be measured using XRF (La, Ce, Pr, Nd and Sm). These elements were compared to the oxalate extractable fraction. In addition, the sample composition (total concentration) was also compared to a set of major and trace elements of the parent material. This set includes SiO_2, TiO_2, Al_2O_3, Fe_2O_3, CaO, MgO, Na_2O, K_2O, MnO, V, Cr, Ni, Cu, Zn, Rb, Sr, Y, Zr, Nb, Ba, Pb, Th und U.

3.5. Stocks calculation and accumulation of pedogenetic products

Organic C and N stocks were calculated according to the following equation:

$$E_{stock,i} = \sum_{a=1}^{n} E_i \Delta z_i \rho_i (1 - RM) \quad (2)$$

where E_{stock} denotes the abundance (kg/m^2) of element i, E_i is the element concentration (kg/t), Δz_i the thickness of layer i (m), ρ_i = soil density (t/m^3) and RM the volumetric mass proportion of rock fragments.

To estimate the amount of pedogenically formed Fe, Al and Mn in soils, the concentrations of each compound in the soil column is compared to the parent material (or the layer with the least concentration). Using the concept of immobile elements, gains and losses of Fe, Al and Mn are derived using equation (3)

$$M_{j,w} = Me_{j,w} \left(\frac{\tau_{j,w}}{1 + \tau_{j,w}} \right) \Delta z_w \rho_w \left(1 - RM\right) \quad (3)$$

With n soil layers, the mass accumulation of the element j is given by:

$$M_{j,w}(\Delta z_w) = \sum_{a=1}^{n} Me_{j,w} \left(\frac{\tau_{j,w}}{1 + \tau_{j,w}} \right) \rho_w \left(1 - RM\right) \Delta z_w \quad (4)$$

where $\tau_{j,w}$ again corresponds to the mass transport function and Δz to the weathered equivalent of the columnar height.

The accumulation of inorganic C was calculated as the overall stock at the position where the parent material did not contain any carbonates. Soils on all the Little Popo Agie terraces (RCTs) and the GalPD terrace of the North Fork, however, contained small amounts of carbonate in the parent materials. In this case, accumulation (or losses) of inorganic C were calculated using the approach given in equations 3 and 4.

4. Results

4.1. General characteristics of the terrace soils

Except for profile RCT2, all investigated soils contain considerable contents of gravel that usually increases with increasing depths (Table 2). The soil texture is mostly clay loam, loam or silt loam.

In some cases (particularly C horizon), the texture can be characterised as sand, loamy sand or sandy (clay) loam. Soil thickness (A+B horizon) varies between 40 and about 150 cm. Due to the presence of carbonates the soils are all neutral or slightly alkaline (often between 7 and 8; Table 3). Only the soils at PB-13-1 and GR-13-2 exhibit slightly acidic conditions in their upper horizons. In several profiles, the B, BC and/or C horizons contain large accumulations of inorganic carbon. The parent material at the RCT and GalPD sites contained some carbonates (13 – 22 g/kg inorg. C). With increasing age of the terraces the average concentration of inorganic carbon increases in each accumulation horizon (from a few g/kg to about 82 g/kg) and also the thickness of the carbonate-rich subsoil horizons (Table 3; Figs. 3 and 4).

In contrast, the concentration of organic carbon shows no trend with age. The influence of organic carbon on total C is manifested almost exclusively in the A horizons. With increasing soil depth the overwhelming proportion of carbon exists in an inorganic form. The C_{org} content in A horizons is not particularly high but is found to a considerable depth. Org. C/N ratios (Table 3) decrease with increasing soil depth and exhibit low values in all profiles, particularly in the subsoils.

Pedogenic oxyhydroxides are present in all profiles. Fe(ox), Al(ox) and Mn(ox) usually decrease with increasing soil depth. In surface soils, oxyhydroxides appear to be enriched passively due to the accumulation of carbonates in the B, BC or C horizon, the weathering of silicate minerals, or blown in as part of the aeolian influx..

4.2. Rare earth elements and normalised elemental contents

We used major and trace elements to assess pathways of chemical weathering and to assess aeolian additions to the terrace soils. To compensate for the dilution effect of accumulated $CaCO_3$, the considered elements were referred to Zr (Fig. 5). For several components (that are not related to carbonates), the 20 ky terrace had the higher values and the 660 ky terrace soils (particularly in the subsoil these differences are pronounced; Fig. 5). Although the terrace soils apparently have

298 received a considerable input of aeolian carbonates over time, some Mg, Ca and K has been lost due
299 to weathering of primary silicates. Mn is depleted in the subsoil but enriched in the A-horizon. In
300 addition, a substantial portion of Na has been leached in the subsoil. Most trace elements are
301 depleted but the signal is quite variable. Finally, Sr has accumulated with time in both A and B(k)
302 horizons. As Sr is strongly linked to the behaviour of Ca (and therefore carbonates) it indicates a
303 more or less continuous aeolian input and translocation of carbonates within the soils.
304 The values of the normalised REEs show that the oxalate-extractable fraction (and thus the fraction
305 found in the weathering products) is three to four orders of magnitude lower than the total REE
306 content. The normalized ratios (with respect to the total contents) are slightly lower in the B
307 horizons than in the A horizons. La, Ce and Nd are enriched over time in the A horizon but depleted
308 in the B(k) horizons. Similarly, the soils older than 20 ky show a slight accumulation of oxalate-
309 extractable REEs in the A horizon and a depletion in the B(k) horizons. This depletion (total and
310 oxalate-extractable fraction) probably is related to a dilution effect due to the accumulation of
311 carbonates in the subsoil.
312 All REE ratios are distinctly lower in the B(k) horizons when compared to the A horizons. As
313 byproducts of weathering, REEs are found to be incorporated into or adsorbed on secondary
314 minerals (clay minerals, pedogenic oxyhydroxides; Laveuf and Cornu, 2009). In the B horizons, the
315 decrease of oxalate-extractable La, Ce, Pr, Nd and Sm with time apparently is caused by dilution
316 owing to the accumulation of carbonates in the Bk horizon. Due to weathering of soil minerals, the
317 normalised oxalate-extractable REE fraction increases in A horizons with time (Fig. 6).
318 To study possible aeolian additions to soils, it is helpful to use chemically immobile elements. We
319 chose the elements Ti, Zr, Nb, Ce, and Y, all of which have a relatively high ionic potential and are
320 considered to be chemically immobile under most near-surface environments (Hutton, 1977; Taylor
321 and McLennan, 1985; Muhs and Benedict, 2006). According to Muhs and Benedict (2006), Tb and
322 Nb are found in ilmenite, rutile, anatase, titanomagnetite, sphene, and biotite. Zr is mostly present in

zircon, although Zr may also be found in other minerals (e.g. zirconolite). The REEs Ce and Y are related to a wide variety of minerals such as phyllosilicates (adsorption on e.g., micas, chlorite, other clay minerals), sphene, amphiboles and apatite (Muhs and Benedict, 2006). Ti/Zr, Ti/Nb and Ce/Y ratios measured in the A horizons, the horizons with carbonate accumulation (Bk, CBk, Ck) and the C horizons show a wide overlap (Fig. 7). The ratios demonstrate that the major chemical background of the various soil horizons does not vary appreciably and suggests that aeolian materials, which should be most concentrated in A and B horizons compared to C horizons, originate predominantly from local sources (e.g. vegetation free proglacial areas or sparsely vegetation-covered areas (Dahms, 1993; Dahms and Applegarth, 2001, 2004). Based on the above relations among the chemical and mineralogical soil properties, the Popo Agie terrace surfaces apparently have received significant amounts of dust that has led to, among other factors, an accumulation of pedogenic carbonate in the profiles over time.

4.3. Soil mineralogy

The primary minerals in the soil profiles are quartz, different types of feldspars, mica and calcite together with 1:1 (kaolinite) and 2:1 (vermiculite) phyllosilicates (Table 4); these mineral suites are consistent with the granitic nature of the local outwash material. 2:1:1 minerals are mostly absent. In addition, the parent materials for soils on the Little Popo Agie and the GalPd (North Fork) terraces contain calcite from the local redbeds. Hematite content also appears to increase with soil age (Table 4, Fig. 8).

4.4. Accumulation of inorganic and organic carbon and pedogenetically formed Fe_{ox}, Al_{ox} and Mn_{ox}

As noted above, the amount of inorganic carbon progressively increases in the soils with age (Fig. 9). This trend exhibits a logistic-curve form: during the first 20 ky the increase is moderate, a stronger increase is seen between 20 ky and 250 ky, and the ratio again slows for the older soils. At

348 the end of the sequence, a considerable amount of inorganic C is stored in the soil with average
349 values of about 60 kg/m^2 in the fine earth fraction. With the exception of the 20 ky terrace soils
350 (where a higher stock was measured with about 14 kg org. C/m^2), the organic carbon stocks were in
351 the range of 8 – 10 kg/m^2. In contrast to inorganic C, the organic carbon stocks did not change over
352 time.
353 The pedogenic stocks of Fe_{ox}, Al_{ox} and Mn_{ox} all change considerably with time (Fig. 10) but the
354 time-trends are not uniform. The Al_{ox} and Mn_{ox} abundances increase until c. 250 ky and then
355 decrease to 660 ky. In contrast, the Fe_{ox} stocks in the soils steadily decrease with increased terrace
356 age, with a marked loss of Fe_{ox} stocks between 5 and 20 ky The stored amount at the start of the
357 time sequence was about 1 kg/m^2; by c. 600 ky the Fe_{ox} stocks decrease to only about 50 g/m^2.
358
359
360 **5. Discussion**
361 *5.1. Carbonate accumulation*
362 Gile et al. (1966, 1981) and Machette (1985) provide baseline data concerning the development of
363 arid-lands soils emphasizing the systematic accumulation of pedogenic carbonate with time on
364 chronosequences of geomorphic surfaces in the southwestern U.S. These authors showed that the
365 calcium contained in pedogenic carbonate of arid-lands soils can derive directly from the parent
366 materials, minerals present in the soil, or from atmospheric additions. As Muhs (2013) indicates,
367 this type of soil development has been recognised in many desert regions of the world where the
368 moisture balance is such that pedogenic carbonates are not fully leached from soil profiles but
369 accumulate slowly, particularly in the subsoil. Where the geologic substrate provides little Ca, the
370 majority of the Ca in pedogenic carbonate derives essentially from aeolian input (Gile et al., 1981;
371 Muhs, 2013). According to McFadden (2013), virtually all calcium in pedogenic carbonate in the
372 southwestern U.S. is derived from calcium-bearing dust that primarily accumulates in a very

373 common horizon of arid land soils – the calcic horizon.

374 The work of McFadden (2013), Reheis (1990; Reheis et al., 1992; Reheis and Kihl, 1995) and
375 Machette (1985) effectively demonstrates the regional importance of carbonate-rich aeolian influx
376 to geomorphic surfaces and the soils that develop in them. Soils reported from the Kyle Canyon
377 fans of Nevada (Reheis et al., 1992), the grassland and forests soils of Saskatchewan (Landi et al.,
378 2003) and various geomorphic surfaces of New Mexico and Utah (Machette, 1985) illustrate the
379 importance of regional carbonate accumulations in soils over time and allow us to generally
380 compare our results to soils developed in other arid regions of the U.S. More locally, Reheis' work
381 (1987) along Rock Creek in the northern Big Horn Basin allows us to compare our results with a
382 similar glacio-fluvial sequence in an adjacent area of the Middle Rocky Mountains.

383 The oldest soils of the Popo Agie River chronosequence are older than those in Nevada (where
384 stocks were available; the oldest Kyle Canyon soil was >800 ka) or Saskatchewan, yet our $CaCO_3$
385 stocks were mid-range between these regions (470 kg $CaCO_3/m^2$ compared to 630 kg/m^2 in the
386 Kyle Canyon fan of Nevada and 134 – 165 kg/m^2 in Saskatchewan).

387 Aeolian influx is the dominant mechanism for the carbonate accumulation over time in the soils
388 developed in the Popo Agie terraces. Calcium from atmospheric deposition enters the soil when it is
389 wetted and moves downward; calcium carbonate is precipitated on drying. Consequently,
390 carbonates tend to accumulate in the lower part of the zone that is wetted (Gile et al., 1981).

391 Reheis et al. (1992) reported that pedogenic $CaCO_3$ accumulated in the arid soils of southern
392 Nevada at a rate of 3 – 15 $g/m^2/y$. Landi et al. (2003) derived $CaCO_3$ accumulation rates from the
393 grassland and forests soils of Saskathewan in the range of 8.3 to 14.3 $g/m^2/y$. In soils of the Rock
394 Creek terraces, Reheis (1987) reported $CaCO_3$ accumulation rates from 0.11 to 5.5 $g/m^2/y$,
395 depending on distance from the range front. The values reported for southern Nevada and
396 Saskatchewan are clearly above those of the present study, but the accumulation rates for the Popo
397 Agie terrace chronosequence (0.19 - 2.13 $g/m^2/y$ using an interval accumulation approach and 0.71

– 1.96 g/m^2/y using a linear approach; Table 5) are within the range of those reported for the Rock Creek terraces, which lie in a similar setting and climatic regime. In Table 5, interval accumulation rates of carbonate and accumulation rates using a 'linear approach' (by dividing the carbonate stocks stored in the soils by the corresponding surface age) are presented. The temporal evolution of the inorganic C abundance in the soils is strongly non-linear (Fig. 9). In soil chronosequences, concentrations or stocks of a component are compared to surface age. The average process rate is often calculated by dividing the measured stocks or concentrations by the soil age (Schlesinger, 1990) – a procedure that in many cases does not reproduce the correct values (because a linear trend is implicitly assumed). A time-split approach or the derivation of a regression curve (having in fact an infinite number of time-splits) would be more precise.

We calculate only a net accumulation rate of $CaCO_3$. The present-day deposition of dust is probably higher and consists of more than just carbonates, but we assume that part of it is leached from the profiles or removed by wind erosion (Hall, 1999; Applegarth and Dahms, 2001). A two-year record of aeolian influx rates in alpine areas of the Wind River Range yielded values of 2.5 – 3.3 g/m^2/y for mineral dust (Dahms and Rawlins, 1996) and Ferrier et al. (2011) estimated even higher long-term dust fluxes (c. 3 to13 g/m^2/y) for the western U.S.

Our results suggest that carbonate accumulation, and by extrapolation dust deposition, has varied over major glacial-interglacial cycles. Carbonate stocks of the Popo Agie soils are the lowest in the younger soils and the highest in the older soils, but the stocks do not increase uniformly over time (Table 5). For example, the average $CaCO_3$ accumulation rate during the 260 to 660 ky period was the lowest (0.19 g/m^2/y; using a linear approach, then the average value between 0 – 660 ky would be 0.71 g/m^2/y; Table 5). The accumulation rate increased to 0.79 g/m^2/y during the 260 – 160 kyr interval, then increased again to 2.13 g/m^2/y from 160 – 20 ky (for the period 0 – 660 ky, the linear approach gives 1.96 g/m^2/y; Table 5), after which the accumulation rate decreased to 0.79 g/m^2/y in the post-glacial (Pinedale – Holocene). Independent of the calculation procedure (interval

423 accumulation or linear approach), highest rates are related to the period 20 – 160 ky BP.
424 A moderately comparable pattern of carbonate accumulation is found in the northern Big Horn
425 Basin (Reheis, 1987). The lowest accumulation rate (0.11 – 1.5 $g/m^2/y$) is reported in soils of the
426 oldest terraces (>400 ky) and the highest rates (1.0 – 5.5 $g/m^2/y$) are estimated from the youngest
427 soils. Machette (1985) reported a similar general pattern of $CaCO_3$ accumulation (older = low;
428 younger = high) from New Mexico and Utah.
429 Carbonate stocks in the Popo Agie terrace soils continue to increase with time but do not appear to
430 reach a quasi-steady state before about 1 My. Reheis (1990) also observed that arid soils develop at
431 linear rates over several 100 ky. In this case soil development reflects progressive dust addition that
432 may be little affected by leaching or erosion. We expect basin soils to accumulate large amounts of
433 Mg and Ca because the climate is dry enough for these soils to retain much of the carbonate derived
434 from aeolian dust (Reheis, 1990).
435
436 *5.2. Chemical weathering pathways*
437 Chemical weathering and leaching of elements are both related to a decreasing value of the open-
438 system mass transport function $\tau_{j,w}$ (negative values represent losses and positive values gains). As
439 we expected, this is in general not the case for Ca, because it is accumulated during pedogenesis.
440 The higher the carbonate content in the soil is, the higher is the corresponding τ_{Ca} (Fig. 11).
441 However, some weathering and leaching of elements do take place. With increasing soil age the
442 carbonate content and τ_{Ca} increase, but the τ_{Na} decreases (Fig. 11). Na predominantly derives from
443 plagioclase and our τ_{Na} values demonstrate that plagioclase is strongly weathered in the older soils -
444 a finding that is also supported by the normalised data of CaO and Na_2O to the parent material (Fig.
445 5). In the Wind River Range, plagioclase is transformed over time into kaolinite, illite and smectite
446 (Mavris et al., 2015). With increasing weathering state, also the REE contents (total and oxalate-
447 extractable content) were mostly higher in the A horizons. Chemical weathering accounts for the

448 largest losses of REEs from the parent material (Laveuf and Cornu, 2009). According to Scarciglia
449 et al. (2009, 2011), weathering of primary minerals and pedogenetic processes give rise to REE
450 adsorption onto reactive sites of organic matter and clay particles. Clay eluviation and illuviation
451 furthermore contribute to the elemental fractionation (Laveuf and Cornu, 2009; Scarciglia et al.,
452 2009, 2011).
453 Under relatively moist conditions, the amounts of pedogenetic, weakly crystalline or amorphous
454 oxyhydroxides increase with time (e.g., Egli et al., 2001; Howard et al., 2012). A similar trend was
455 detected in the wetter, cooler high altitude subalpine-to-alpine environments of the Wind River
456 Range (Dahms et al., 2012). With progressing soil evolution portions of the amorphous forms may
457 be transformed into goethite (FeOOH; cf., Ellis and Atherton, 2003). In sharp contrast, the
458 abundance of pedogenetically formed Fe_{ox} (weakly crystalline and amorphous forms) in the Popo
459 Agie terrace soils decreased strongly with increasing time (Fig. 9). Some of the weakly crystalline
460 Fe may also derive from aeolian input – its contribution, however, does not seem to be that high
461 because no clear Fe accumulation with time was detected (Fig. 5). We suggest that, due to the semi-
462 arid climate, a relatively fast transformation of weakly crystalline and amorphous Fe-forms into
463 crystalline Fe-oxides or -hydroxides (that are not dissolved using oxalate) is likely. This idea is
464 supported by the XRD results: more hematite (Fe_2O_3) is detected in the older soils (Table 4; Fig. 8)
465 whereas goethite seems to be nearly absent (presumably due to the dry climatic conditions). This
466 weathering relationship is further supported by Quinton et al. (2011) who demonstrated that the
467 absolute and relative hematite abundance in the Little Popo Agie soils (profiles RCT-2-to-5)
468 increased with soil age. Aeolian influx of crystalline Fe-minerals does not seem to be a major
469 process contributing to such a change, because no distinct accumulation (nor depletion) of Fe was
470 detected (Fig. 5).
471 The pedogenetically-formed Fe stocks of the Holocene soil (PB-13-1) corresponds to what has been
472 measured at alpine moraine sites of the Wind River Range (Dahms et al., 2012). At cooler and

473 moister sites (montane-to-alpine) the formation of Fe_{ox} continues over time, whereas the
474 transformation of weakly- and poorly-crystalline phases into crystalline forms is enhanced at the
475 terrace sites.
476 Stocks of pedogenic Al-forms in the Popo Agie soils tend to increase with time. This is an expected
477 result of the weathering process; however, the stocks remain at a rather low level even after several
478 100 ky (200-300 g/m^2) suggesting modest weathering compared to alpine moraine soils of the WRR
479 (Dahms et al., 2012).
480 Gile et al. (1981) observed that in arid environments the amount of organic carbon generally
481 increases with the clay content. Our observations show that the relation between organic carbon and
482 clay and silt stocks is rather weak (Fig. 12). We see a higher correspondence, however, between
483 nitrogen and silt. We do not really understand why, but we hypothesise that larger amounts of
484 highly-charged phyllosilicates are available in the silt fraction that enable better adsorption of
485 organic matter (having proteinaceous compounds) and protection from microbial decay. The higher
486 amount of highly-charged phyllosilicates could be related to silt-sized mineral grains (e.g.,
487 plagioclase, feldspar and micas) that are weathered in situ to clay minerals. Kleber et al. (2007),
488 Kögel-Knabner et al. (2008) and others show the importance of the mineral fraction in OM
489 protection. According to Kleber et al.'s model the formation of particularly strong organo-mineral
490 associations is favoured in the so-called 'contact zone' in situations where proteinaceous materials
491 unfold upon adsorption and thus increase the adhesive strength by adding hydrophobic interactions
492 to electrostatic binding. This could be a reason why such low C/N ratios have been measured in our
493 soils. In addition, more aggregates simply may be formed by silt that physically protects organic
494 compounds from decay. Another explanation for the very low C/N ratio particularly in the deeper
495 soil horizons, might be due to the exceptionally high accumulation of nitrate beneath the active
496 rooting zone (Graham et al., 2008; Menon et al, 2010). According to these authors, soil resources
497 (water and organic carbon), precipitation, net dryfall and rare leaching events are the primary

498 factors that lead to accumulation of NO_3^--N particularly in this region. Previous measurements of
499 N-deposition in the WRR (Galbraith et al., 1991) showed that a considerable portion of NO_3^--N is
500 imported from upwind sources (presumably) west of the WRR.
501
502 *5.3. Climatic inferences*
503 Reheis (1987) observed that the 'Basin Soils' located farthest from the range front preserve the
504 most complete record of climate change along the Rock Creek chronosequence. The use of
505 alternating clay cutans and $CaCO_3$ layering from thin-section analyses enables Reheis to infer
506 alternations of glacial/interglacial climates in these soils. The inference is that climate fluctuations
507 over time here were enough to cause these changes, but not enough to destroy previously-developed
508 soil characteristics – hence the continuous accumulation of carbonate (regardless of rate) over time.
509 Such features have often a polygenetic origin. Clay increase and cause of clay orientation is often
510 not due to a single genetic process or event (Gunal and Ransom, 2006).
511 The Popo Agie River soils occur in a similar environment, and so most likely also reflect climate
512 fluctuations over the past c. 700 kyrs. We did not thin-section our soils and so do not have data
513 similar to those of Reheis (1987). Reheis concluded that it is likely that the variable depths of clay
514 and carbonate in the older Rock Creek terraces soils were most likely a result of increases in
515 wetting depth due to an increase in available water capacity (AWC) coincident with the addition of
516 aeolian fines over time rather than to changes in overall climate variability (e.g., higher
517 precipitation levels during interglacial periods). Overall, the Rock Creek soils data suggest an
518 overall pattern of less precipitation during glacial periods. Alternately, Nettleton and Chadwick
519 (1991) suggested that moisture conditions during the Pleistocene in the lower Wind River Basin
520 near Riverton were not appreciably different from those at present and also suggest that dust
521 deposition rates have not appreciably changed.

522 Our $CaCO_3$ accumulation data are similar to those for Rock Creek and it seems reasonable that
523 some carbonates in the soils would be dissolved during periods of greater moisture. However, our
524 results suggest that $CaCO_3$ accumulates most effectively in the soils of the western Wind River
525 Basin during the cool, windy glacial periods rather than during warmer, less windy interglacials
526 (Table 5). Hall and Jaworowski (1999) have suggested that A horizons of Bull Lake-age are thinner
527 and Bt horizons are closer to the surface than on soils of nearby Pinedale moraines due to erosion
528 caused by the cold foehn winds off the local valley glaciers. Studies of Greenland and the Antarctic
529 ice cores show that MIS glacial stages are drier and windier (and thus dustier) than interglacials
530 (e.g., Fuhrer et al., 1999; Svensson et al., 2000). Thus, it seems reasonable to assume that more Ca-
531 rich materials normally are in flux in a glaciated region during time periods that are predominately
532 glacial than during warmer periods. It appears that, on average, our soil $CaCO_3$ accumulation rates
533 (and associated aeolian deposition rates) were the highest during MIS 6-2 (c. 160 ky; Cohen and
534 Gibbard, 2011). Note that the time-span 160-to-20 ky predominantly covers cold MIS phases. The
535 other time-split periods (660-to-260 ky and 260-to-160 ky) include a comparatively larger
536 proportion of warm (interglacial) phases. Machette's (1985) model for long-term carbonate
537 accumulation shows that soils in locations with climatic regimes similar to that of the Popo Agie
538 (Buena Vista & Boulder/Denver, Colorado) fall into the 'influx limited' region of the model
539 (Machette, 1985). This model suggests that the variations observed in the Rock Creek, Wind River,
540 and Popo Agie soils are more likely to be caused by variations in aeolian influx under the influence
541 of climate variability than either influx rates or glacial/interglacial climate variations acting alone.
542 This reasoning should include a decrease in vegetation cover during glacial periods. We suggest
543 that change in rates of soil carbonate accumulation does not exclusively indicate a climate signal
544 but probably is overprinted by limits to the supply of sediments, the availability of aeolian material,
545 balanced by the effect(s) of increasing loss by erosion of fines as the surfaces age and the
546 decreasing ability of the surface soil to accumulate more eolian fines as pore spaces fill with

infiltrated silt and clay. These factors may well influence the (apparently) decreasing accumulation rates detected in the older soils.

6. Conclusions

Chronosequences are a fundamental tool for studying and representing change in Earth surface systems. Increasingly, chronosequences are understood to be much more complex than a simple monotonic progression from a starting point to a stable end-state (Phillips, 2015). In this case, the soil physical and chemical characteristics combined with the presumed age associations allow us to derive interval accumulation rates of $CaCO_3$ that appear to show varying rates of dust deposition over several glacial-interglacial cycles The development trajectories thus show a certain sensitivity to disturbances and changes (Phillips, 2015).

The well-preserved terraces along the Popo Agie River of the southeastern Wind River Range allows us to develop a relative-age chronosequence for soil development on (mostly) granitic alluvium and to compare soil development here with soils on similar terrace sequences elsewhere in the western U.S. Carbonate stocks in the fine earth of the soils increase with increasing soil age and are thought to be related to aeolian influx over time and influenced by the major cycles of mid-to-late Pleistocene climate change represented in our chronosequence [Holocene, Pinedale (20 ky), early and late Bull lake (160 and 260 ky) and Sacagawea Ridge (c. 660 ky)]. By inference of the carbonate stocks, aeolian influx of inorganic carbon apparently was lowest in this area during the period of c. 260 – 660 ky and the highest during the period of c. 160 – 20 ky.

A quasi-steady state situation (where inputs of materials to the soil system and outputs via erosion and weathering are almost equal) does not appear to have been reached by 660 ky. The change in carbonate accumulation rates in the soils may exclusively indicate a climate signal but is probably

571 also related to a supply limitation of sediments, the subsequent disposability of aeolian material,
572 and increasing erosion of older soil surfaces.
573 We suggest a scenario where the long-term carbonate accumulation rates in soils of Quaternary
574 glacial, alluvial, and glacio-fluvial sequences of this region are controlled through the rates of
575 aeolian influx over time as modified by glacial/interglacial climate variations rather than by
576 glacial/interglacial variations in moisture availability. Thus we consider the carbonate accumulation
577 rates in these soils to be 'influx limited' rather than 'moisture limited' (Machette, 1985) so that the
578 *soil-forming regime* of these soils is more closely related to that of the semi-arid Rocky Mountain-
579 Intermountain region than to the arid southwest of New Mexico, Arizona, and southern Nevada and
580 California.
581 Compared to other published results, the carbonate accumulation rates determined for the Wind
582 River Range terraces were relatively low. Despite the dominance of carbonate accumulation as a
583 pedogenetic process, chemical weathering and leaching of primary minerals occurred (e.g.
584 plagioclase weathering coupled with a subsequent Na release). In addition, pedogenetic Al and Mn
585 have formed, but at relatively low rates when compared to moister and cooler conditions in the
586 Wind River Range. Due to the dry climate, weakly crystalline and amorphous Fe-forms seemed to
587 be transformed relatively quickly into crystalline forms (hematite). With increasing age, inorganic
588 carbon (with an average at the oldest sites of 60 kg C_{inorg}/m^2) becomes the lion's share of the stored
589 total carbon. Organic carbon remained relatively at a stable level (about 8 – 10 kg C_{org}/m^2) over the
590 entire soil formation phase.
591
592
593 **7. Acknowledgements**
594 We would like to thank S. Röthlisberger and M. Kovacic for their help in the laboratory at the
595 University of Zürich. Students in the Environmental Sediment Analysis class (Geog4220) at the

University of Northern Iowa helped Dahms to develop the data for % $CaCO_3$. We are, furthermore, indebted to Marith C. Reheis and an unknown reviewer for their helpful comments on an earlier version of the manuscript.

References

Anders, M.H., Saltzman, J., Hemming, S.R., 2009. Neogene tephra correlations in eastern Idaho and Wyoming: Implications for yellowstone hotspot-related volcanism and tectonic activity. Geol. Soc. Am. Bull. 121, 827-856.

Applegarth, M.T., Dahms, D.E., 2001. Soil catenas of calcareous tills, Whiskey Basin, Wyoming, USA. Catena 42, 17-38.

Applegarth, M.T., Dahms, D.E. 2004. Aeolian modification of moraine soils, Whiskey Basin, Wyoming, USA. Earth Surf. Proc. Land. 29, 579-585.

Bierman, P.R., Montgomery, D.R., 2014. Key Concepts in Geomorphology. W.H. Freeman, NY.

Birkeland, P.W., 1973. Use of Relative Age-Dating Methods in a Stratigraphic Study of Rock Glacier Deposits, Mt. Sopris, Colorado. Arct. Alp. Res. 5, 401-41.

Birkeland, P.W., Burke, R.M., Shroba, R.R., 1987. Holocene Alpine Soils in Gneissic Cirque Deposits, Colorado Front Range. U.S. Geol. Surv. Bull. 1590-E.

Birkeland, P. W., Machette, M., Haller, K., 1991. Soils as tool for applied Quaternary geology. Miscellaneous Publication 91–3, Utah Geological and Mineral Survey.

Blackwelder, E., 1915. Post-Cretaceous history of the mountains of western Wyoming. J. Geol. 23, 302-340.

Boulding, B.H., Boulding, J.R., 1981. Genesis of Silty and Clayey Material in Some Alpine Soils in the Teton Mountains, Wyoming and Idaho. Indiana Acad. Sci. Proc. 91, 552-562.

620 Chadwick, O.A., Brimhall, G.H., Hendricks, D.M., 1990. From a black to a grey box - A mass
621 balance interpretation of pedogenesis. Geomorphology 3, 369-390.
622 Chadwick, O.A., Hall, R.D., Phillips, F.M., 1997. Chronology of Pleistocene glacial advances in the
623 central Rocky Mountains. Geol. Soc. Am. Null. 109, 1443-1452.
624 Cohen, K.M., Gibbard, P., 2011. Global chronostratigraphical correlation table for the last 2.7
625 million years. Subcommission on Quaternary Stratigraphy (International Commission on
626 Stratigraphy), Cambridge, England.
627 Colman, S.M., Pierce, K.L., 1986. The glacial sequence near McCall, Idaho--weathering rinds, soil
628 development, morphology, and other relative-age criteria. Quat. Res. 25, 25-42.
629 Dahms, D.E., 1993. Mineralogical evidence for eolian contribution to soils of late Quaternary
630 moraines, Wind River Mountains, Wyoming, USA. Geoderma 59, 175-196.
631 Dahms, D.E., 2002. Glacial Stratigraphy of Stough Creek Basin, Wind River Range, Wyoming.
632 Geomorphology 42, 59-83.
633 Dahms, D.E, 2010. Soils and glacial stratigraphy of the Popo Agie River Basin, southern Wind
634 River Range, Wyoming. Abstracts with Programs, #180207 (Paper No. 95-4), Geological
635 Society of America Annual Meeting, 31 Oct-3 Nov, Denver, CO.
636 Dahms, D.E., 2004a. Glacial limits in the middle and southern rocky Mountains, USA, south of the
637 Yellowstone Ice Cap. In: Ehlers, J., Gibbard, P.L. (Eds.), Quaternary Glaciations – Extent &
638 Chronology, Part II: North America. Developments in Quaternary Science, Vol 2b. Elsevier,
639 Amsterdam, pp. 269-282.
640 Dahms, D.E., 2004b. Relative and numeric age data for Pleistocene glacial deposits and diamictons
641 in and near Sinks Canyon, Wind River Range, Wyoming, U.S.A. Arct. Antarct. Alp. Res. 36, 59-
642 77.
643 Dahms, D.E., Rawlins, C.L., 1996. A two-year record of eolian sedimentation in the Wind River
644 Range, Wyoming, U.S.A. Arct. Alp. Res. 28, 210-216.

645 Dahms, D. Favilli, F., Krebs, R., Egli, M., 2012. Soil weathering and accumulation rates of oxalate-
646 extractable phases from alpine chronosequences of up to 1 Ma in age. Geomorphology 151-152,
647 99-113.
648 Dixon, J., 1992. Alpine and Subalpine Soil Properties as Paleoenvironmental Indicators. Phys.
649 Geog. 12, 370-384.
650 Egli, M., Fitze, P. Mirabella, A., 2001. Weathering and evolution of soils formed on granitic,
651 glacial deposits: results from chronosequences of Swiss alpine environments. Catena, 45, 19-47.
652 Ellis, S., Atherton, J.K., 2003. Properties and development of soils on reclaimed alluvial sediments
653 of the Humber estuary, eastern England. Catena 52, 129-147.
654 Fabel, D., Harbor, J., Dahms, D., James, A., Elmore, D., Horn, L., Daley, K., Steele, C., 2004. Spa-
655 tial patterns of glacial Erosion at a valley scale derived from terrestrial cosmogenic ^{10}Be and ^{26}Al
656 concentrations in rock. Ann. Assoc. Am. Geogr. 94, 241–255.
657 Ferrier, K.L., Kirchner, J.W., Finkel, R.C., 2011. Estimating millennial-scale rates of dust
658 incorporation into eroding hillslopes regolith using cosmogenic nuclides and immobile
659 weathering tracers. J. Geophys. Res. 116, F03022.
660 Fuhrer, K., Wolf, E.W., Johnsen, S.J., 1999. Timescales for dust variability in the Greenland Ice
661 Core Project (GRIP) ice core in the last 100,000 years. J. Geophys. Res. – Atmos. 104 (D24),
662 31043–31052.
663 Galbraith, A.F., Harrelson, C.C., and Rawlins, C., 1991. Acid deposition in the Wind River
664 Mountains. Air Quality Related Values Report 2, Bridger-Teton National Forest, Jackson,
665 Wyoming, 48p.
666 Gile, L.H., Peterson, F.F., Grossman, R.B., 1966. Morphological and genetic sequences of
667 carbonate accumulation in desert soils. Soil Sci. 101, 347–360.

668 Gile, L.H., Hawley, J.W., Grossman, R.B., 1981. Soils and geomorphology in the Basin and Range
669 area of Southern New Mexico – Guidebook to the Desert Project. New Mexico Bureau of Mines
670 & Mineral Resources, Memoir 39, University of New Mexico Printing Plant, Socorro.
671 Gosse, J.C., Evenson, E.B., Klein, J., Sorenson, C., 2003. Cosmogenic nuclide glacial
672 geochronology in the Wind River Range, Wyoming. In: Easterbrook, D.J. (Ed.), Quaternary
673 Geology of the United States. INQUA 2003 Field Guide Volume, 2003 INQUA Congress.
674 Desert Research Institute, Reno, Nv, pp. 49-56.
675 Graham, R.C., Hirmas, D.R., Wood, Y.A., Amrhein, C., 2008. Large near-surface nitrate pools in
676 soils capped by desert pavement in the Mojave Desert, California. Geology 36, 259-262.
677 Gunal, H, Ransom, M.D., 2006. Clay illuviation and calcium carbonate accumulation along a
678 precipitation gradient in Kansas. Catena 69, 59-69
679 Hall, R.D., 1999. Effects of Climate Change on Soils in Glacial Deposits, Wind River Range,
680 Wyoming. Quat. Res. 51, 248-261.
681 Hall, R.D., Shroba, R.R., 1995. Soil evidence for a glaciation intermediate between the Bull Lake
682 and Pinedale glaciations at Fremont Lake, Wind River Range, Wyoming. Arct. Alp. Res. 27, 89-
683 98.
684 Hall, R.D., Jaworowski, C., 1999. Reinterpretation of the Cedar Ridge section, Wind River Range,
685 Wyoming: Implications for the glacial chronology of the Rocky Mountains. Geological Society
686 of America Bulletin 111, 1233-1249.
687 Hancock, G. S., R.S. Anderson, O.A. Chadwick and R.C. Finkel, 1999. Dating fluvial terraces with
688 ^{10}Be and ^{26}Al profiles: application to the Wind river, Wyoming. Geomorphology 27, 41-60.
689 Hitz, C., Egli, M., Fitze, P., 2002. Determination of the sampling volume for representative analysis
690 of alpine soils. Z. Pflanz. Bodenkunde 165, 326-331.
691 Howard, J.L., Clawson, C.R., Daniels, W.L., 2012. A comparison of mineralogical techniques and
692 potassium adsorption isotherm analysis for relative dating and correlation of Late Quaternary

693 soil chronosequences. Geoderma 179-180, 81-95.
694 Hutton, J. T., 1977. Titanium and zirconium minerals. In: Dixon, J. B., Weed, S. B. (Eds.), Minerals
695 in Soil Environments. Madison, Wisconsin, Soil Science Society of America, pp. 673–688.
696 Jackson, M. L., 1969. Soil Chemical Analysis: Advanced Course. Department of Soil Science,
697 University of Wisconsin, Madison.
698 Jaworowski, C., 1992. A probable new Lava Creek ash locality: implication for Quaternary
699 geologic studies in the western Wind River Basin, Wyoming, USA. Contributions to Geology,
700 University of Wyoming 29, 111-117.
701 Kleber, M., Sollins, P., Sutton, R., 2007. A conceptual model of organo-mineral interactions in
702 soils: self-assembly of organic molecular fragments into zonal structures on mineral surfaces.
703 Biogeochemistry 85, 9-24.
704 Klute, A., 1986. Methods of Soil Analysis: Part 1, Physical and Mineralogical Methods, 2nd ed.
705 Madison, WI: American Society of Agronomy.
706 Kögel-Knabner, I., Guggenberger, G., Kleber, M., Kandeler, E., Kalbitz, K., Scheu, S., Eusterhues,
707 K., Leinweber, P., 2008. Organo-mineral associations in temperate soils: Integrating biology,
708 mineralogy, and organic matter chemistry. J. Plant Nutr. Soil Sc. 171, 61-82.
709 Landi, A., Mermut, A.R., Anderson, D.W., 2003. Origin and rate of pedogenic carbonate
710 accumulation in Saskatchewan soils, Canada. Geoderma 117, 143-156.
711 Laveuf, C., Cornu, S., 2009. A review on the potentiality of Rare Earth Elements to trace
712 pedogenetic processes. Geoderma 154, 1-12.
713 Litaor, M., 1987. The Influence of Eolian Dust on the Genesis of Alpine Soils in the Front Range,
714 Colorado. Soil Sci. Soc. Am. Jour. 51, 142-147.
715 Litaor, M., 1988. Reply to Comments on 'The Influence of Eolian Dust on Alpine Soils.' Soil Sci.
716 Soc. Am. J. 52, 301-302.

717 Machette, M.N., 1985. Calcic soils of the southwestern United States. In: Weide, D.L. (Ed.), Soils
718 and Quaternary Geology of the Southwestern United States. Geological Society of America
719 Special Paper 203, pp. 1-21.
720 Marchand, D.E., 1970. Soil Contamination in the White Mountains, eastern California. Geol. Soc.
721 Am. Bull. 81, 2497-2506.
722 Massatti, R.T., 2007. A floristic inventory of the east slope of the Wind River Mountain Range and
723 vicinity, Wyoming. PhD Thesis, University of Wyoming, ProQuest, UMI Dissertations
724 Publishing.
725 Mavris, C., G. Furrer, D. Dahms, S.P. Anderson, A. Blum, J. Goetze, A. Wells, M. Egli, 2015.
726 Decoding potential effects of climate and vegetation change on mineral weathering in alpine
727 soils: An experimental study in the Wind River Range (Wyoming, USA). Geoderma 255-256,
728 12-26.
729 McFadden, L.D., 2013. Strongly dust-influenced soils and what they tell us about landscape
730 dynamics in vegetated aridlands of the southwestern United States. Spec Pap Geol Soc America
731 500, 501-532.
732 McKeague, J.A., Brydon, J.E., Miles, N.M., 1971. Differentiation of forms of extractable iron and
733 aluminium in soils. Soil Sci Soc Am Proc 35, 33-38.
734 Mears, B., 1974. The evolution of the Rocky Mountain glacial model. In: Coates, D.R. (Ed.),
735 Glacial Geomorphology. SUNY-Binghamton, NY, pp. 11-40.
736 Menon, M., Parratt, R.T., Kropf, C.A., Tyler, S.W., 2010. Factors contributing to nitrate
737 accumulation in mesic desert vadose zones in Spanish Springs Valley, Nevada (USA). J Arid
738 Environ 74, 1033-1040.
739 Mizota, C., van Reeuwijk, L.P., 1989. Clay mineralogy and chemistry of soils formed in volcanic
740 material in diverse climate regions. International Soil Reference and Information Centre, Soil
741 Monograph, vol. 2. Wageningen.

742 Mourier, B., Poulenard, J., Chauvel, C., Faivre, P., Carcaillet, C., 2008. Distinguishing subalpine
743 soil types using extractible Al and Fe fractions and REE geochemistry. Geoderma 145, 107–120.
744 Muhs, D.R., 2013. The geologic records of dust in the Quaternary. Aeolian Research 9, 3-48.
745 Muhs, D.R., Benedict, J.B., 2006. Eolian additions to late Quaternary alpine soils, Indian Peaks
746 Wilderness Area, Colorado Front Range. Arct. Antarct. Alp. Res. 38, 120-130.
747 Muhs, D.R., Bush, E.A., Stewart, K.D., Rowland, T.R., Crittenden, R.E., 1990. Geochemical
748 evidence of Saharan dust parent material for soils developed on Quaternary limestones of
749 Caribbean and western Atlantic islands. Quat. Res. 33, 157-177.
750 Muhs, D.R., Benedict, J.B. and Evans, J., 1992. Sources of Probable Eolian Sediments on Late
751 Quaternary Alpine Moraines, Colorado Front Range: Evidence from Trace Element
752 Geochemistry. Abstracts of the 12th Biennial Mtg., AMQUA, Davis, Calif., August 24-26.
753 Muhs, D.R., Prins, M.A., Machalett, B., 2014. Loess as Quaternary paleoenvironmental indicator.
754 PAGES Magazine 22, 84-85.
755 Nettleton, W.D., Chadwick, O.A., 1991. Soil-landscape relationships in the Wind River Basin,
756 Wyoming. The Mountain Geologist 28, 3-11.
757 Phillips, F.M., Zreda, M., Gosse, J., Klein, J., Evenson, E., Hall, R.D., Chadwick, O.A., Sharma, P.,
758 1997. Cosmogenic ^{36}Cl and ^{10}Be ages of Quaternary glacial and fluvial deposits of the Wind
759 River Range, Wyoming. Geol. Soc. Am. Bull. 109, 1453-1463.
760 Phillips, D.J., 2015. The robustness of chronosequences. Ecol. Model. 298, 16-23.
761 Picard, M.D., 1993. The early Mesozoic history of Wyoming. In: Snoke, A.W., Steidtmann, J.R.,
762 Roberts, S.M. (Eds.), Geology of Wyoming, Geological Survey of Wyoming Memoir #5, pp.
763 210-248.
764 Pierce, K.L., 2004. Pleistocene glaciations in the Rocky Mountains. In: Gillespie, A.R., Porter,
765 S.C., Atwater, B.F. (Eds.), The Quaternary Period in the United States. Developments in
766 Quaternary Science 1, Jim Rose (Series Ed.). Elsevier, Amsterdam, pp. 63-76.

767 PRISM Climate Group, 2014. Annual average precipitation (1981-2010). Oregon State University.
768 Quinton, E.E., Dahms, D.E., Geiss, C.E., 2011. Magnetic analyses of soils from the Wind River
769 Range, Wyoming, constrain rates and pathways of magnetic enhancement for soils from
770 semiarid climates. Geochem. Geophys. Geosyst. 12, Q07Z30.
771 Reheis, M.C., 1987. Soils in granitic alluvium in humid and semiarid climates along Rock Creek,
772 Carbon County, Montana: U.S. Geological Survey Bulletin 1590-D.
773 Reheis, M.C., 1988. Replacement of silicate grains by $CaCO_3$ in semiarid soils of south-central
774 Montana, U.S.A. Geoderma 41, 243-261.
775 Reheis, M.C., 1990. Influence of climate and eolian dust on the major-element chemistry and clay
776 mineralogy of soils in the northern Bighorn Basin, U.S.A. Catena 17, 219-248.
777 Reheis, M. C., Kihl, R., 1995. Dust deposition in southern Nevada and California, 1984-1989:
778 Relations to climate, source area, and source lithology. J. Geophys. Res. 100 (D5), 8893-8918.
779 Reheis, M.C., Sowers, J.M., Taylor, E.M., McFadden, L.D., Harden, J.W., 1992. Morphology and
780 genesis of carbonate soils on the Kyle Canyon fan, Nevada, U.S.A. Geoderma 52, 303-342.
781 Richmond, G.M., 1948. Modification of Blackwelder's sequence of Pleistocene glaciation in the
782 Wind River Mountains, Wyoming. Geol. Soc. Am. Bull. 59, 1400-1401.
783 Richmond, G.M., 1964. Three pre-Bull Lake tills in the Wind River Mountains, Wyoming: A
784 reinterpretation. U.S. Geol. Surv. Prof. Paper 501-D, 104-109.
785 Richmond, G.M., 1973. Geologic Map of the Fremont Lake South quadrangle, Sublette County,
786 Wyoming. U.S. Geological survey, Geologic Quadrangle Map GQ-1138.
787 Richmond, G.M., 1986. Stratigraphy and correlation of glacial deposits of the Rocky Mountains,
788 the Coorado Plateau & the ranges of the Great Basin. Quat. Sci. Rev. 5, 99-127.
789 Richmond, G.M., 1987. Type Pinedale Till in the Fremont Lake area, Wind River Range,
790 Wyoming. Geological Society of America Centennial Field Guide – Rocky Mountain Section,
791 pp. 201-204.

792 Sauer, D., Schellmann, G., Stahr, K., 2007. A soil chronosequence in the semi-arid environment of
793 Patagonia (Argentina). Catena 71, 382-393.
794 Scarciglia, F., Barca, D., De Rosa, R., Pulice I., 2009. Application of laser ablation ICP-MS and
795 traditional micromorphological techniques to the study of an Alfisol (Sardinia, Italy) in thin
796 sections: Insights into trace element distribution. Geoderma 152, 113-126.
797 Scarciglia, F., Tuccimei, P., Vacca, A., Barca, D., Pulice, I., Salzano, R., Soligo, M., 2011. Soil
798 genesis, morphodynamic processes and chronological implications in two soil transects of SE
799 Sardinia, Italy: Traditional pedological study coupled with laser ablation ICP-MS and
800 radionuclide analyses. Geoderma 162, 39-64.
801 Schlesinger, W. H., 1990. Evidence from chronosequence studies for a low carbon-storage potential
802 of soils. Nature 348, 232–234.
803 Shroba, R.R., Birkeland, P.W., 1983. Trends in Late Quaternary Soil Development in the Rocky
804 Mountains and Sierra Nevada of the western United States. In: Wright, H.E. (Editor), Late
805 Quaternary Environments of the United States, Volume I. The Late Pleistocene. Univ. of Minn.,
806 Minneapolis, pp.145-156.
807 Singer, M. J., Janitzky, P., 1986. Field and laboratory procedures used in a soil chronosequence
808 study. U.S. Geological Survey Bulletin, 1648.
809 Soil Survey Division Staff. 1993. Soil survey manual. Soil Conservation Service. U.S. Department
810 of Agriculture Handbook 18.
811 Soil Survey Staff, 2014. Keys to Soil Taxonomy, 12th ed. USDA-Natural Resources Conservation
812 Service, Washington, DC.
813 Sorenson, C.J., 1987. Soils Map of the Fremont Lake South Quadrangle, Sublette County,
814 Wyoming. U.S. Geol. Surv., Misc. Invest. Map I-1800.
815 Sun, S.S., McDonough, W.F., 1989. Chemical and isotopic systematics of oceanic basalts:
816 implications for mantle composition and processes. In: Saunder, A.D., Norry, M.J. (Eds.),

817 Magmatism in Oceanic Basins. Geological Society of London, Special Publication 42, London,
818 pp. 313–345.
819 Svensson, A., Biscaye, P.E., Grousset, F.E., 2000. Characterization of late glacial continental dust
820 in the Greenland Ice Core Project ice core. J. Geophy. Res. 105 (D4), 4637-4656.
821 Swanson, D.K., 1985. Soil Catenas on Pinedale and Bull Lake Moraines, Willow Lake, Wind River
822 Mountains, Wyoming. Catena 12, 329-342.
823 Taylor, S.R., McLennan, S.M., 1985. The Continental Crust: Its Composition and Evolution.
824 Blackwell, Oxford.
825 Thorn, C.E., Darmody, R.G., 1980. Contemporary Eolian Sediments in the Alpine Zone, Colorado
826 Front Range. Phys. Geog. 1, 162-171.
827 US Climate Data, 2015 (online). http://www.usclimatedata.com/climate/lander/wyoming/united-
828 states/uswy0101
829 Vandenberghe, J., 2015. River terraces as a response to climatic forcing: Formation processes,
830 sedimentary characteristics and sites for human occupation. Quatern. Int. 370, 3-11.
831 Williams, J., 1973. Neoglacial Chronology of the 4th of July Cirque, Central Colorado Front
832 Range: Discussion. Geol. Soc. Am. Bull. 84, 3761-3765.

Figure captions

Fig. 1. Location of the Popo Agie Basin on the southeastern flank of the Wind River Range in west-central Wyoming. Note the three forks of the Popo Agie grade to the Wind River south of Riverton in the central Wind River Basin and that the Wind River becomes the Big Horn River at the northern mouth of Wind River Canyon (located just north of the lake at the mid-upper right of the image (Google Earth Pro).

Fig. 2. Location of the studied terrace elements and associated soil profiles along each of the three forks of the Popo Agie River: A) the North Fork, B) the Middle Fork (together with the airport terrace AT (Jaworowski, 1992); see text), C) the Little Popo Agie (Red Canyon), D) terraces of RCT2-5 in Little Popo Agie and E) view toward the north from RCT-4 (Little Popo Agie). Photos generally are SE-to-NW (for A) to C)). The terrace/soil locations are within 2.3 miles of the mouth of North Fork Canyon, 5.0 miles from the mouth of Sinks Canyon (Middle Popo Agie) and within 0.5 mile of the mouth of Little Popo Agie Canyon.

Fig. 3. Investigated soil profiles with designated horizons. For RCT5, the inset shows the character of the Bkm (cemented 'petrocalcic') horizon of the U.S. Soil Taxonomy.

Fig. 4. A) Average concentration of inorganic and B) total carbon as a function of soil depth and age. Values are averages of the soils within the corresponding age classes.

Fig. 5. Spider diagram of normalised (to the parent material = PM) A) major elements in the A horizon, B) trace elements in the A horizon, C) major elements in the B(k) horizon and D) trace elements in the B(k) horizon. The concentrations are given as a function of surface age.

To account for the dilution effect of $CaCO_3$, the contents were ratioed to the immobile element Zr:

$$\text{Conc. measured(norm)/Conc. PM (norm)} = \frac{\frac{C_s}{Zr_s}}{\frac{C_{PM}}{Zr_{PM}}}$$ where C_s = element concentration of the sample, Zr_s = Zr concentration of the sample, C_{PM} = element concentration of PM (parent material) and Zr_{PM} = Zr concentration of PM.

Fig. 6. Normalised (to the parent material = PM) REE concentrations for some selected profiles as a function of terrace age. The total content and the oxalate-extractable fraction of selected REEs are shown for A) the A-horizon and B) the B(k)-horizon. The content of Sm in the A horizon was below the XRF detection limit.

Fig. 7. Binary diagram of concentration ratios of A) Ti/Zr vs Ti/Nb and B) Ti/Zr vs Ce/Y for samples of the topsoil, the horizons with carbonate accumulation (Bk, CBk, Ck) and the C horizon from the various sites.

Fig. 8. X-ray diffraction pattern for three samples from the soils PB-13-2 (Bw horizon), GR-13-1 (Btk) and PB-13-1 (AB horizon) having different ages. The diffraction peaks associated with quartz (Q), calcite (Cc) and hematite (H) are labelled.

Fig. 9. A) Inorganic and B) organic carbon stocks (average ± standard deviation) as a function of age (± estimated error range).

Fig. 10. Average (±SD) accumulation (abundance) of pedogenetically formed A) Fe, B) Al and C) Mn in the entire profiles as a function of terrace age (± error range).

Fig. 11. A) Comparison of the relative losses or gains (open system mass transport function τ) of Ca with the carbonate content and B) relative mass changes of Ca vs. Na.

Fig. 12. Comparison of organic C stocks with the abundance of A) clay and B) silt of the individual soil horizons. Significant correlations only exist between C) N stocks and clay abundance and D) N and silt abundance.

Figure 1

Click here to download high resolution image

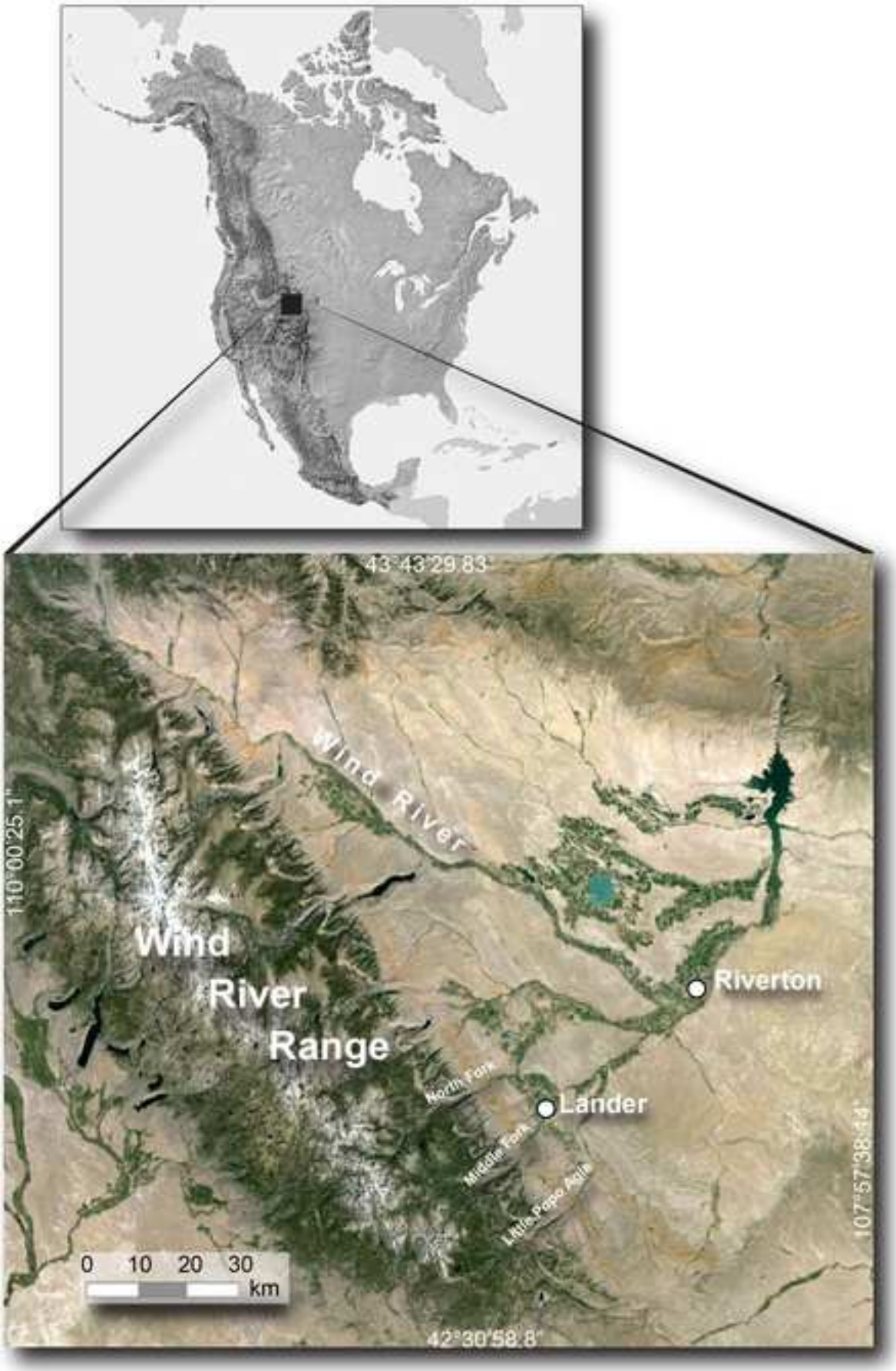

Figure 2
Click here to download high resolution image

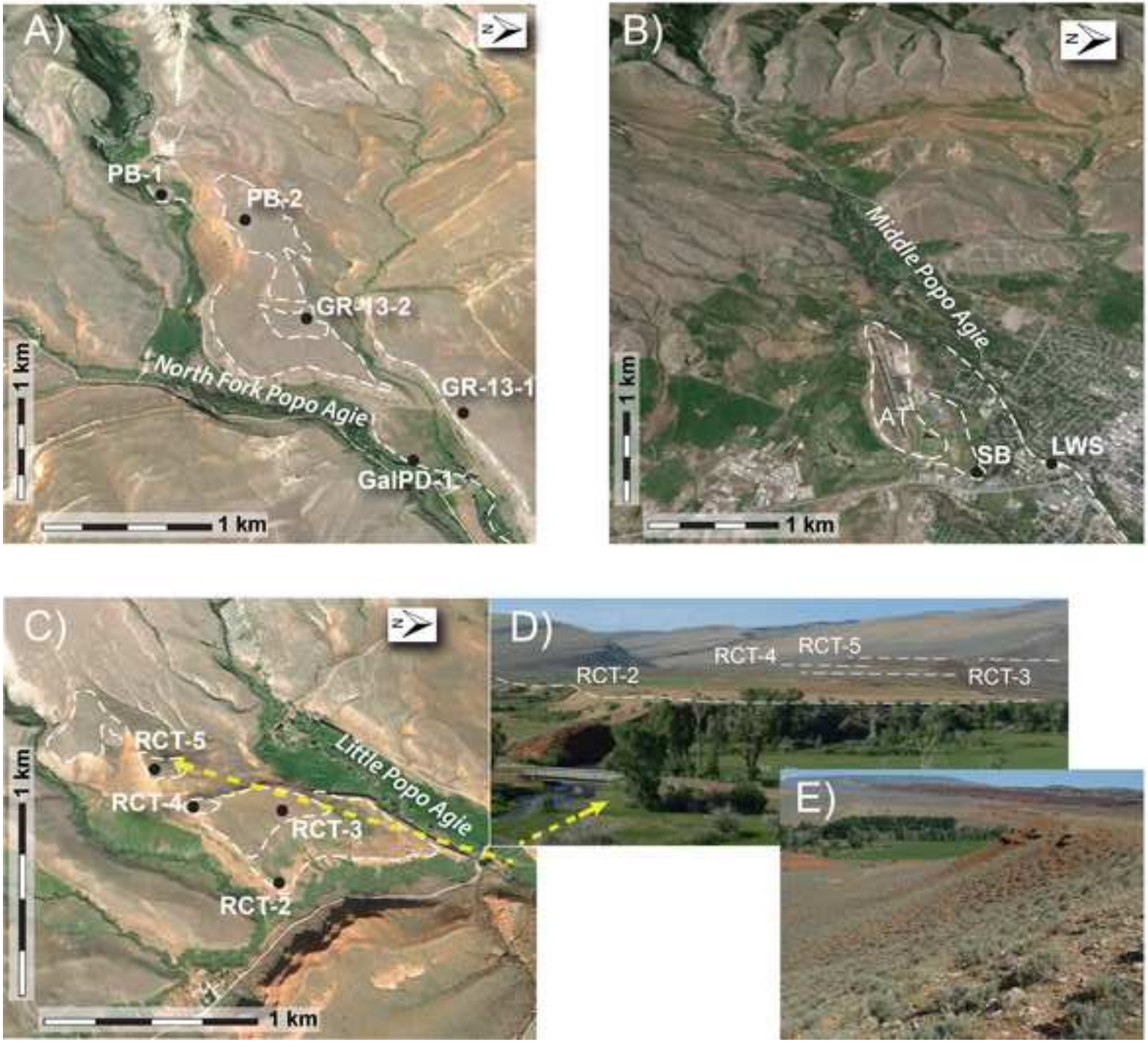

Figure 3

Click here to download high resolution image

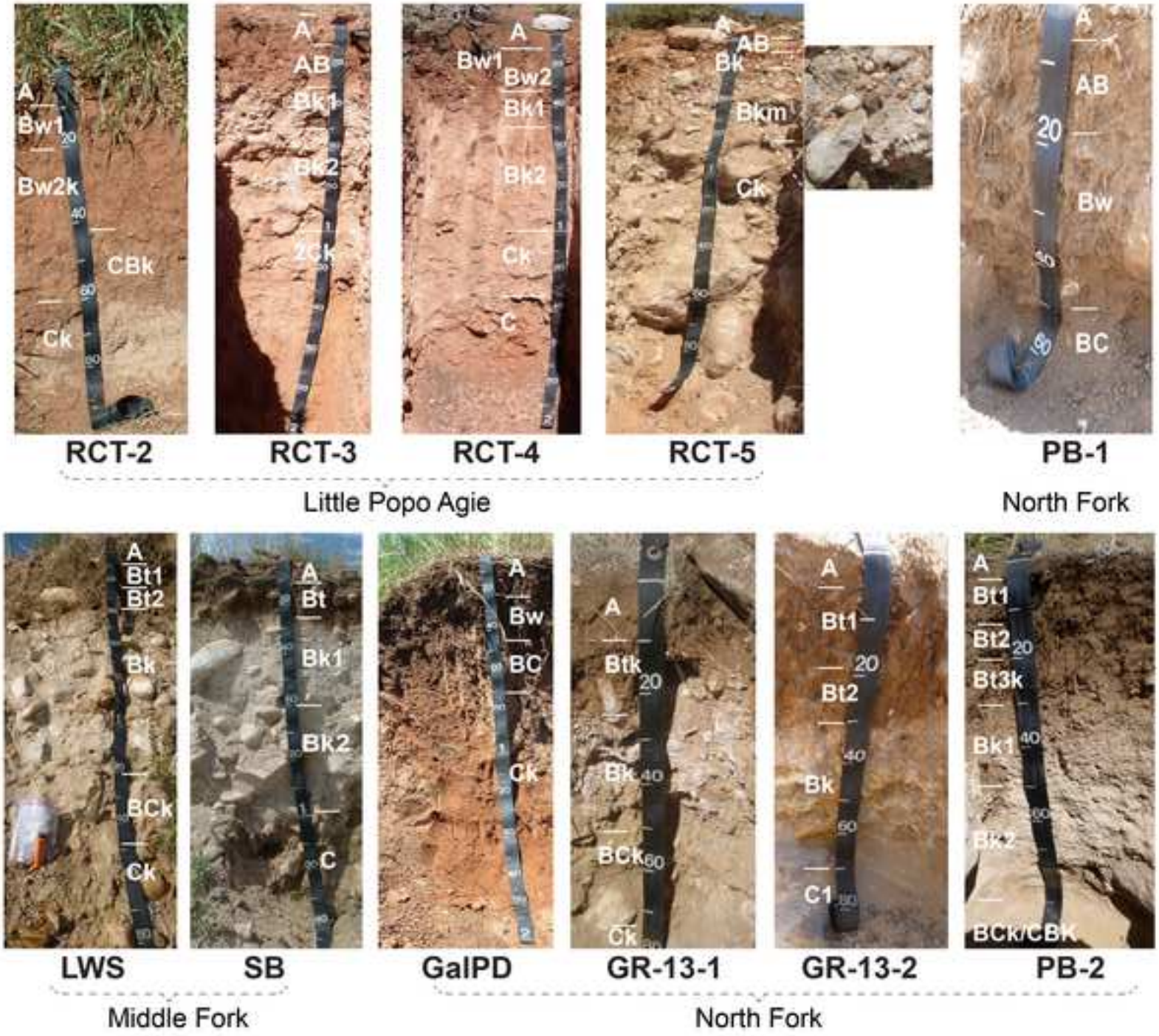

Figure 4

Click here to download high resolution image

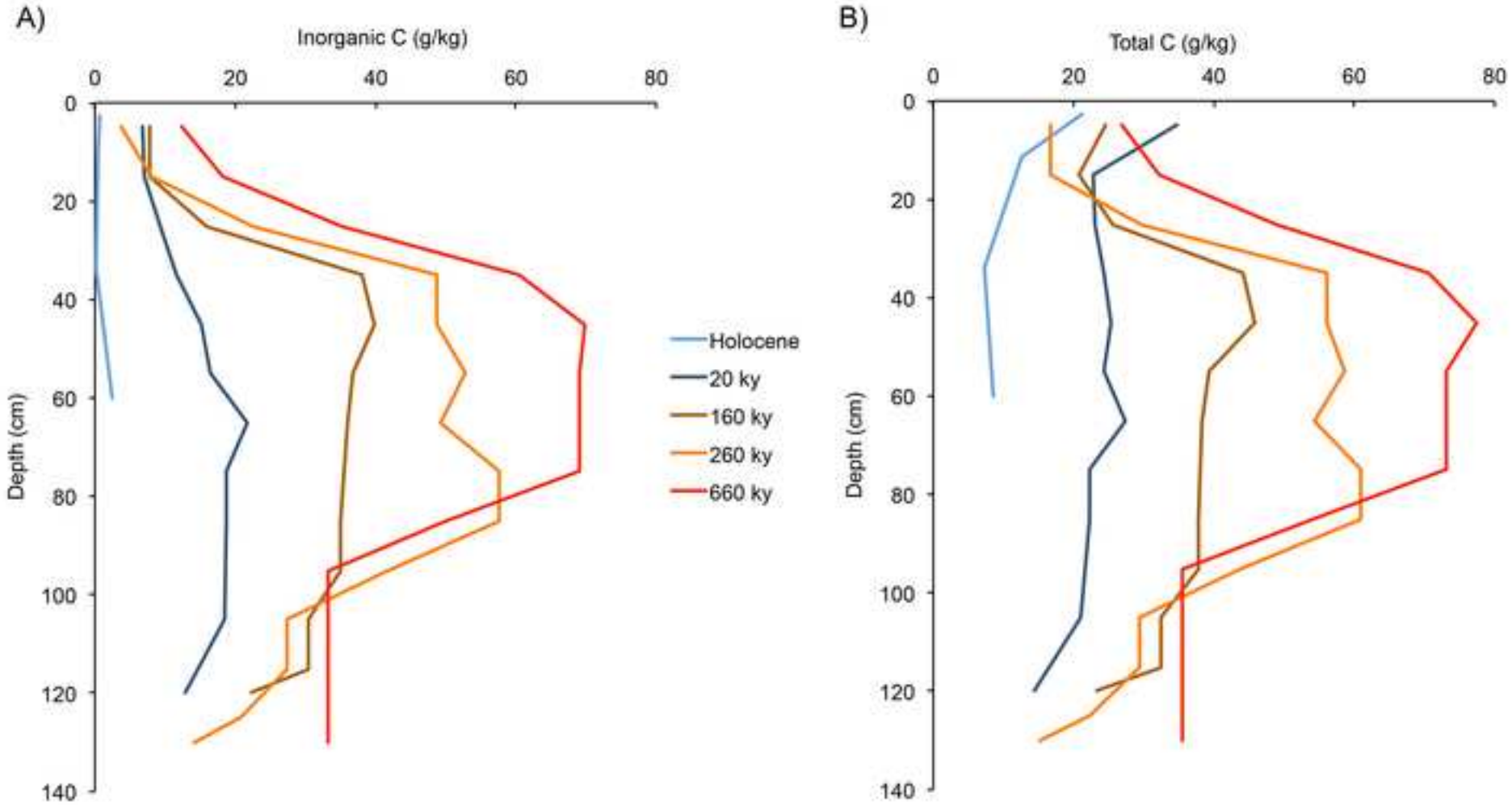

Figure 5

Click here to download high resolution image

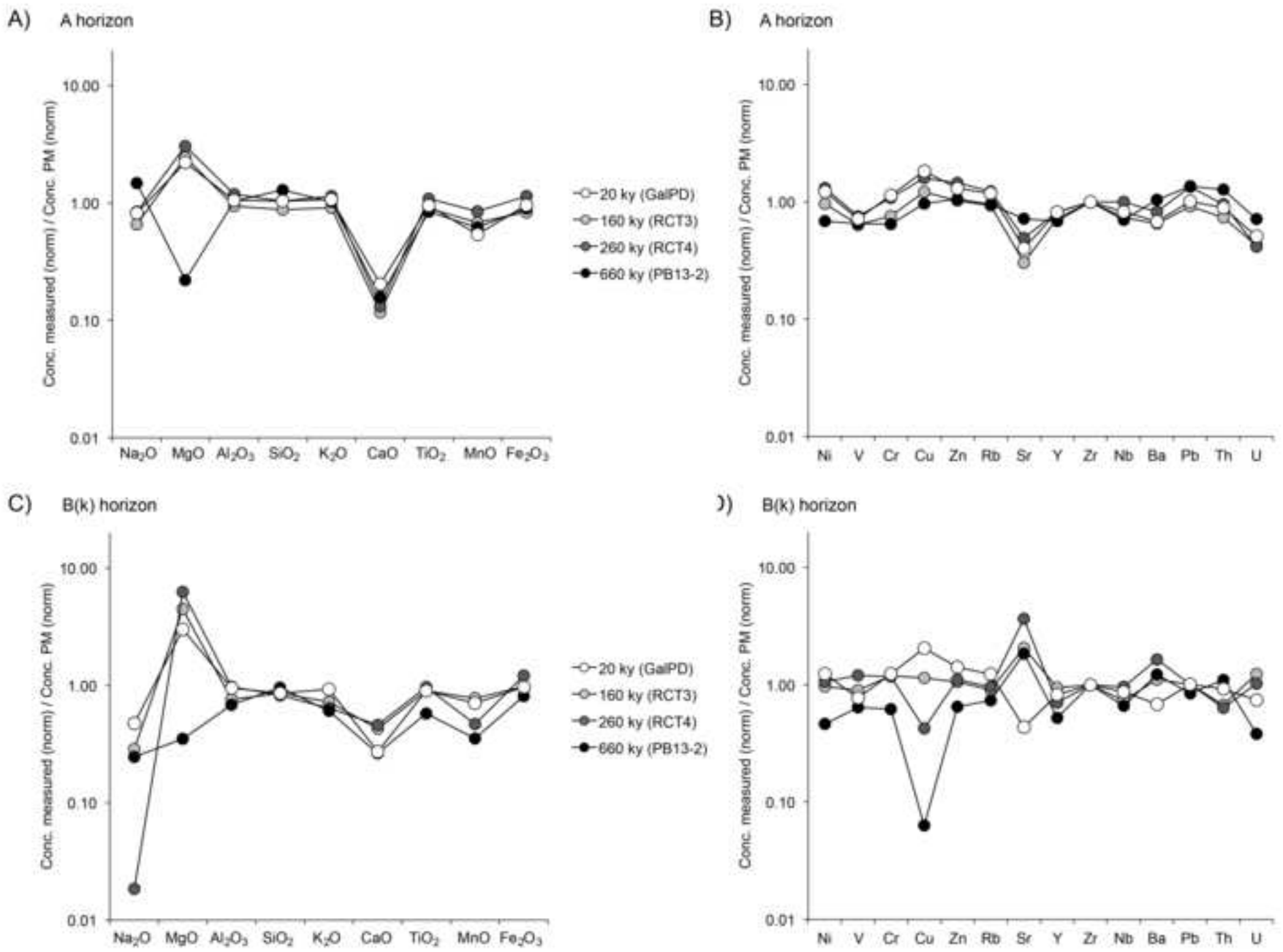

Figure 6

Click here to download high resolution image

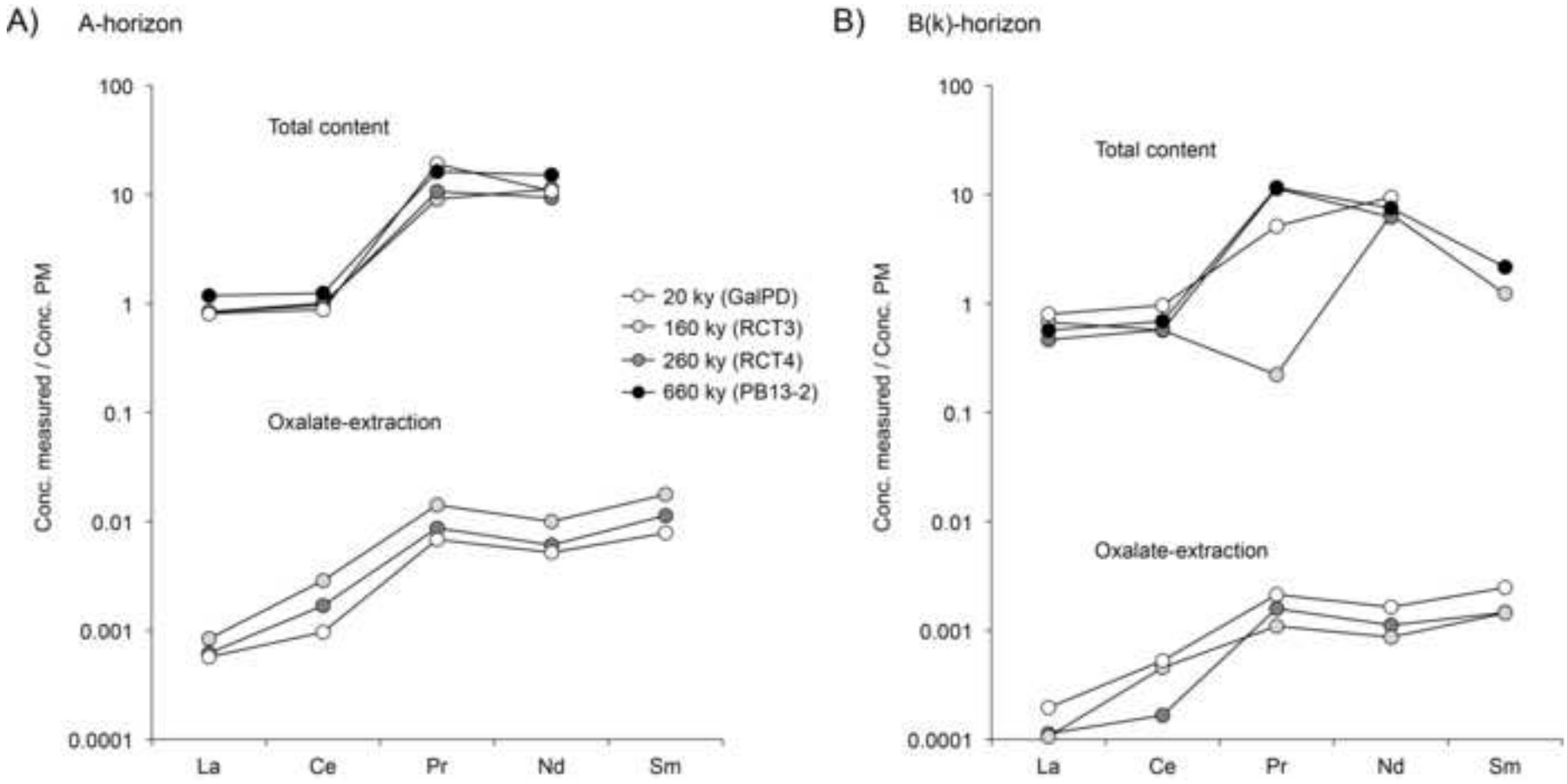

Figure 7

Click here to download high resolution image

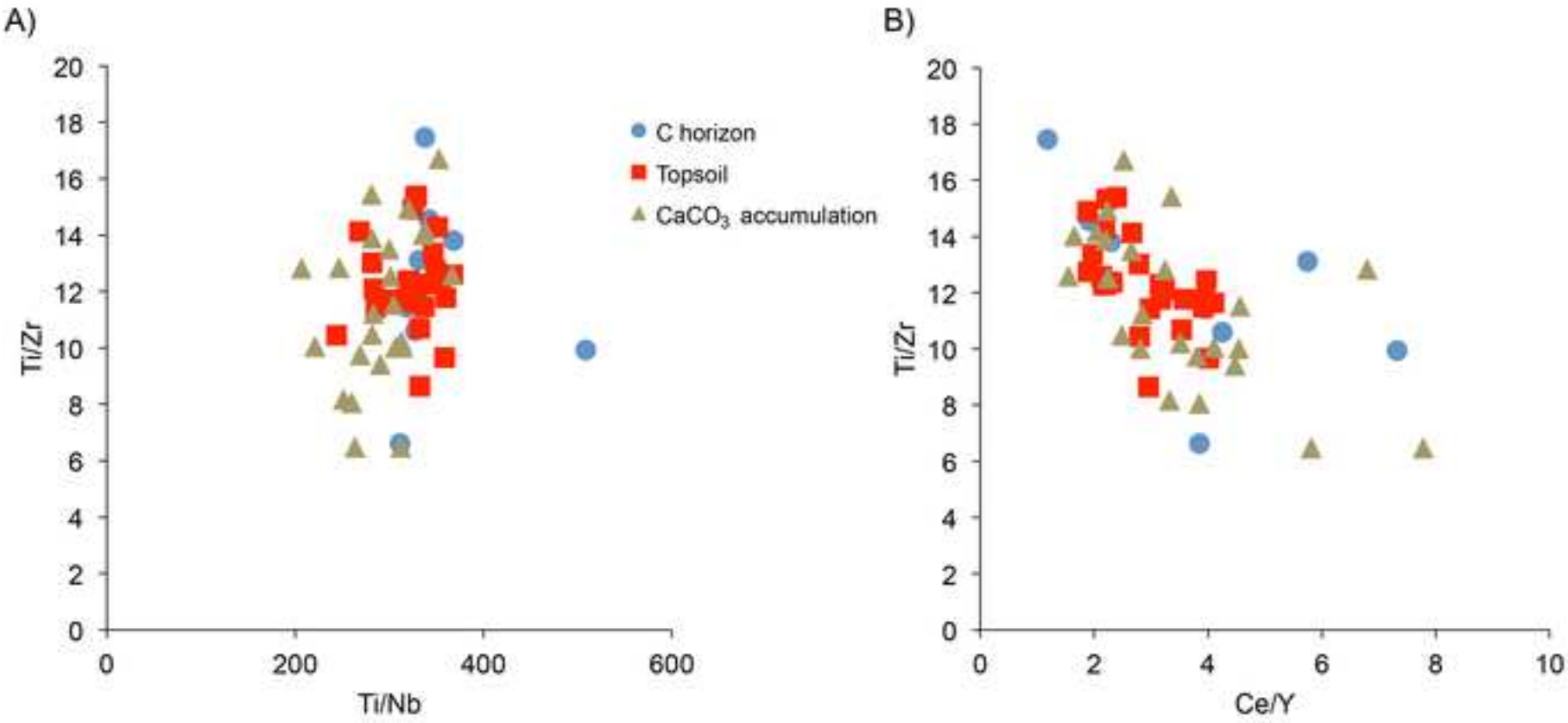

Figure 8

Click here to download high resolution image

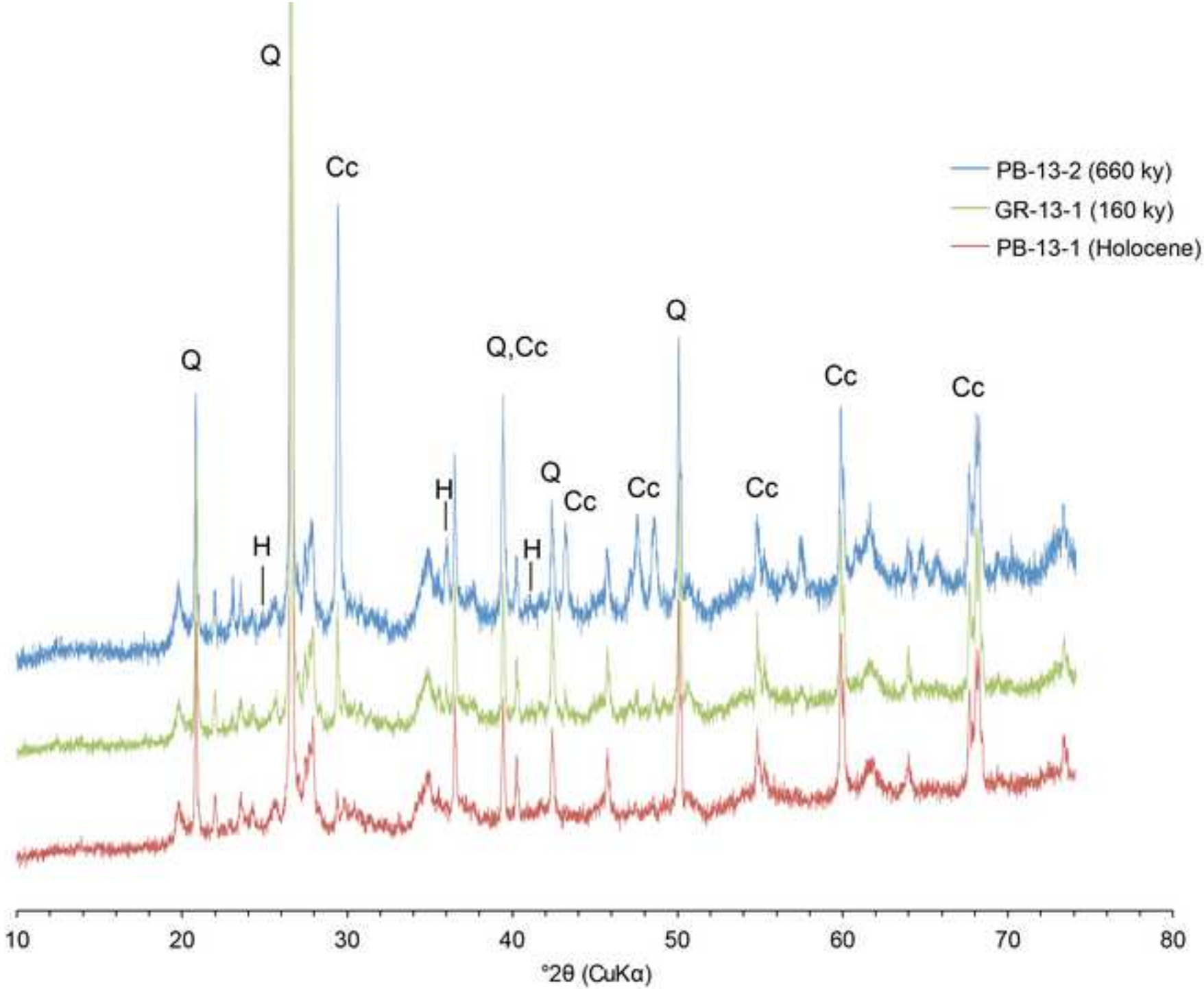

Figure 9
Click here to download high resolution image

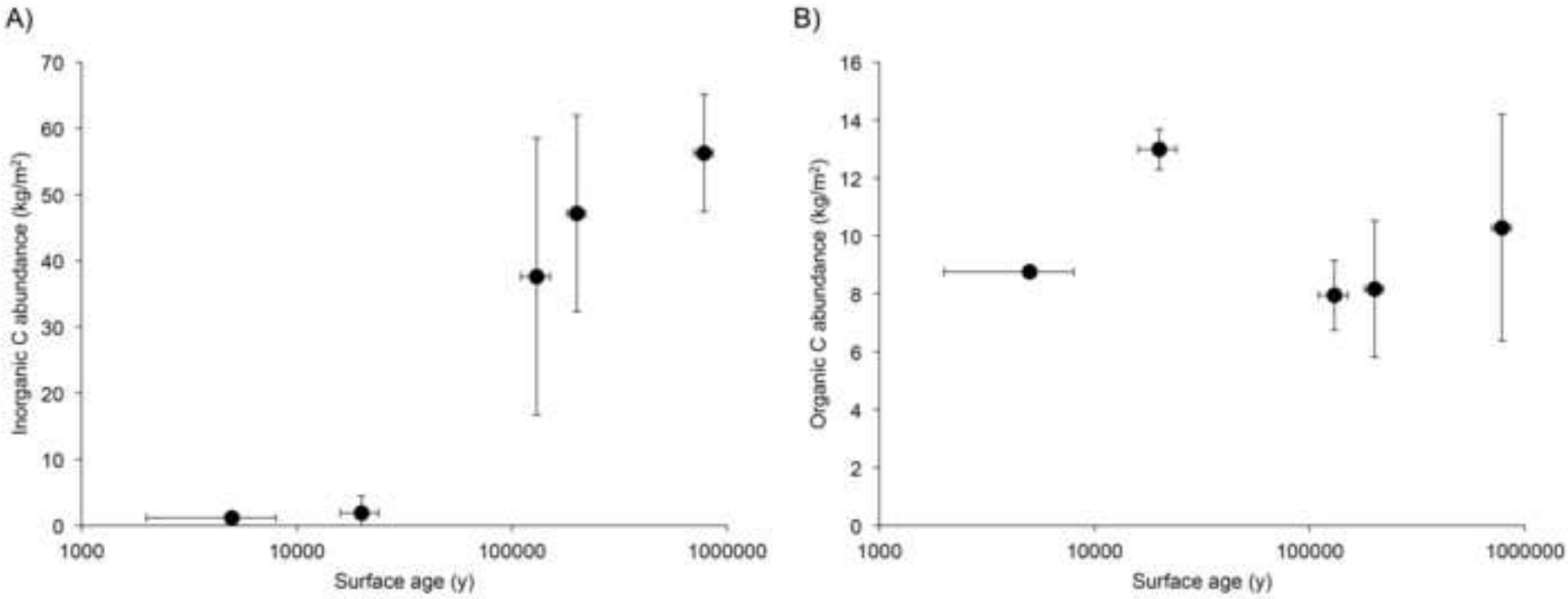

Figure 10
Click here to download high resolution image

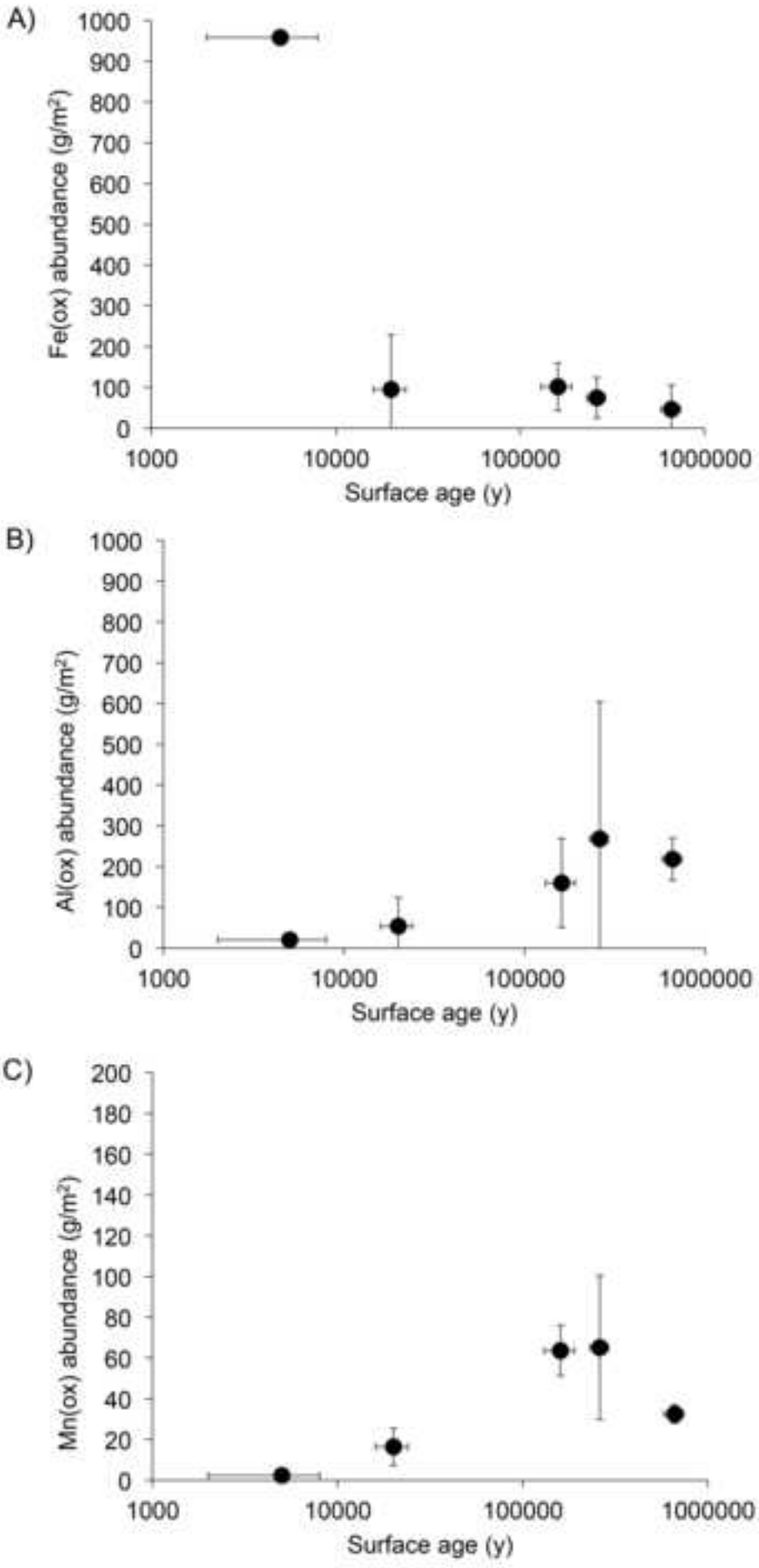

Figure 11

Click here to download high resolution image

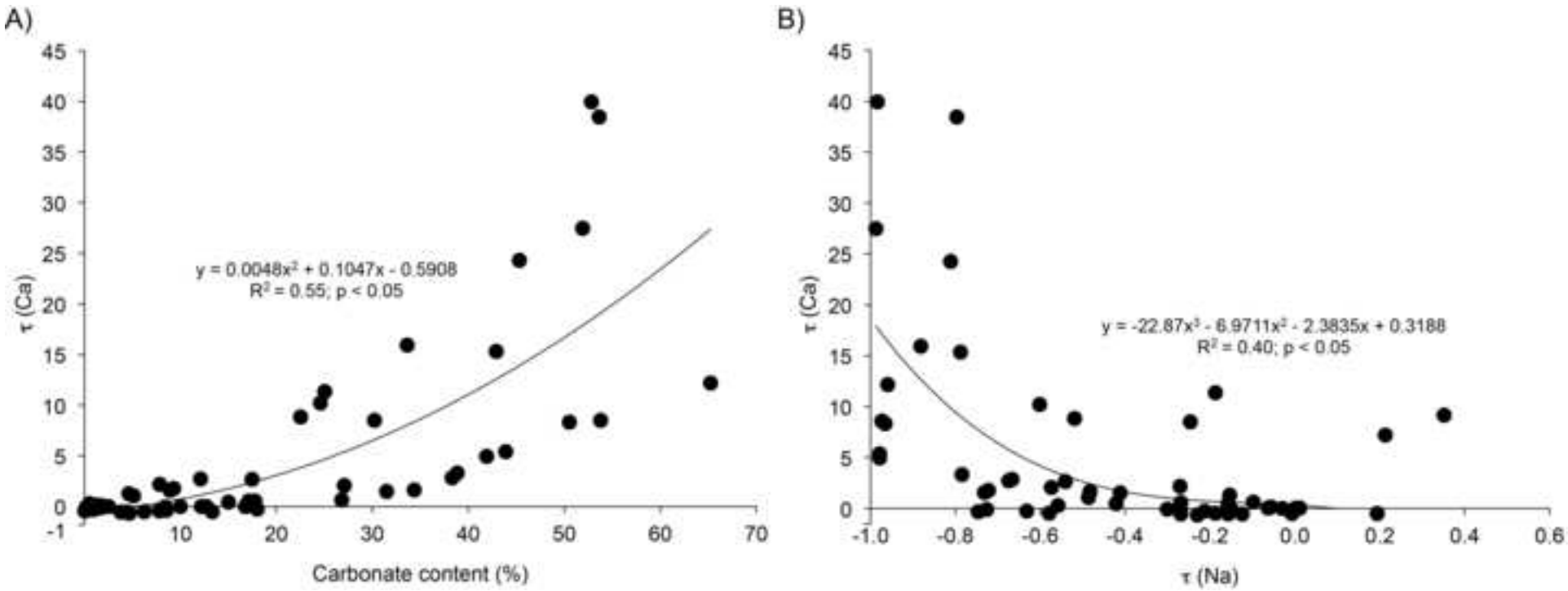

Figure 12

Click here to download high resolution image

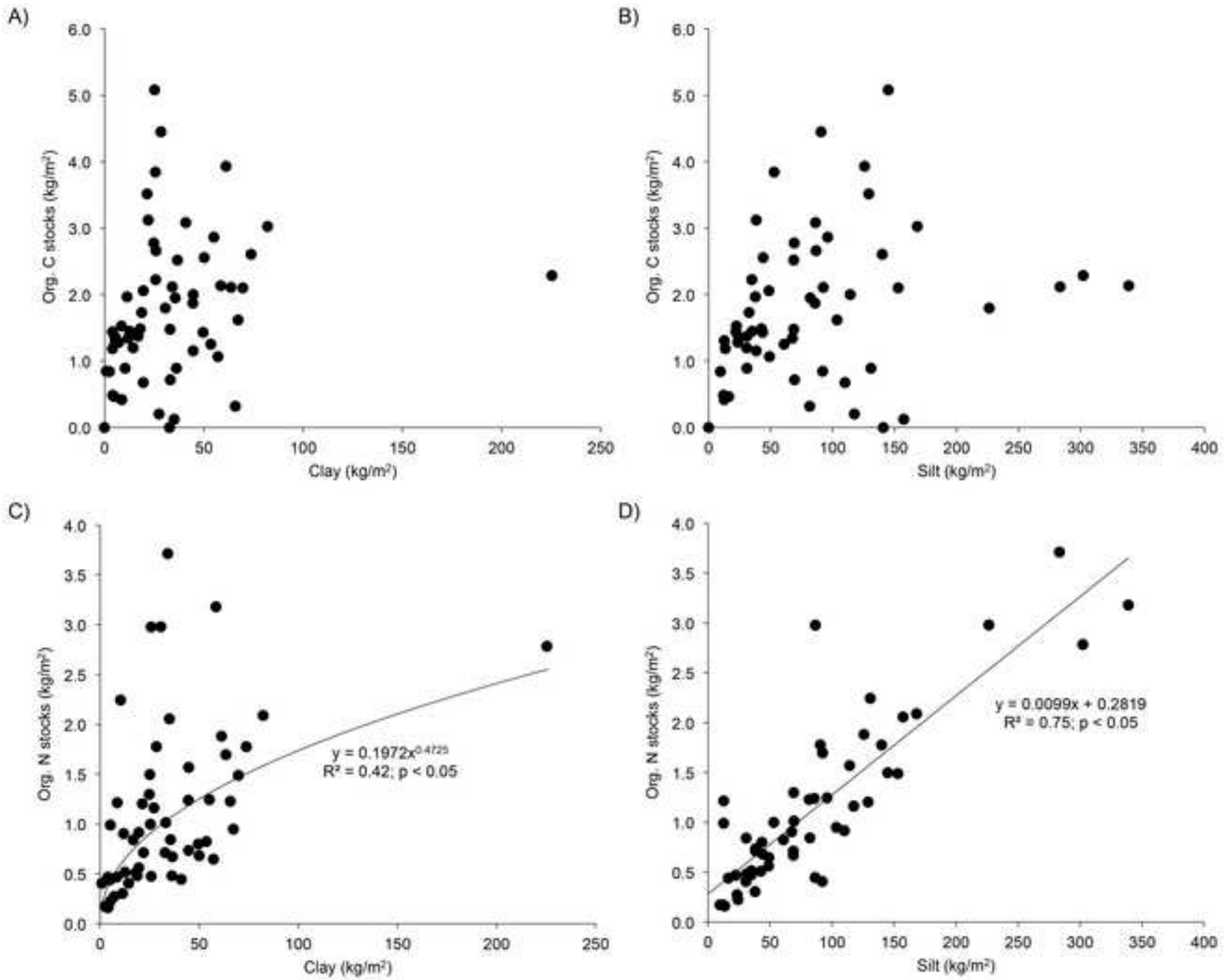

Table 1
Click here to download Table: Table_1.doc

Table 1. Characteristics of the terrace sites along the North Fork, Middle Fork and Little Popo Agie rivers, Wind River Range.

Site / Soil profile	Longitude °E	Latitude °N	Elevation m asl	Parent Material*	Vegetation	Terrace age[1)] ky	MAP[2)] mm/year	MAT[2)] °C
Little PopoAgie – Red Canyon								
RCT2	108°39'54"	42°40'39"	1722	RP/C	Grass, Sagebrush	20 (±4)	250-380	6.7
RCT3	108° 40'10"	42°40'40"	1750	RP/C	Grass, Sagebrush	160 (±30)	250-380	6.6
RCT4	108° 40'10"	42°40'24"	1768	RP/C	Grass, Sagebrush	260 (±30)	250-380	6.4
RCT5	108° 40'19"	42°40'17"	1795	RP/C	Grass, Sagebrush	660 (±40)	250-380	6.3
Middle Fork - Lander								
LWS-13-1	108° 43'34"	42°49'47"	1643	G	Grass, Sage, riparian	160 (±30)	330	7.2
SB	108°43'12"	42°49'30"	1676	G	Grass, Sagebrush	260 (±30)	330	7.0
North Fork								
PB-13-1	108°53'16"	42°52'08"	1826	OG	Grass, Sage, riparian	5 (±3)	250-380	6.1
GalPD	108°51'39"	42°53'03"	1768	RP/C	Grass, Sage, riparian	20 (±4)	250-380	6.4
GR-13-1	108°51'47"	42°53'12"	1798	G	Grass, Sagebrush	160 (±30)	250-380	6.3
GR-13-2	108°52'15"	42°52'46"	1838	G	Grass, Sagebrush	260 (±30)	250-380	6.0
PB-13-2	108°52'58"	42°52'28"	1908	G	Grass, Sagebrush	660 (±40)	250-380	5.6

[1)] Ages for the ~5, ~20, ~160 and ~260 ky terraces are assigned (a) according to their local morphostratigraphic positions and (b) their correlations to previously-dated terrace units along the Wind/Bighorn river (heights above the modern channels and associated incision rates (Chadwick et al., 1997; Dahms 2010; Hancock et al., 1999; Nettleton and Chadwick, 1991; Phillips et al., 1997; Reheis, 1987). The highest terraces (soils RCT5, PB-13-2) were assigned an age of ~660 ky according to their correlation to the 'Airport' terrace of the Middle Fork ('AT' of Fig. 2B), in which an ash deposit of Lava Creek age previously was reported (Anders et al., 2009; Jaworowski, 1992).
[2)] Data source: Massatti (2007), Dahms et al. (2012), PRISM Climate Group (2014)
*G = granitic alluvium; RP/C = Red Peak/Chugwater fines over coarse granitic gravels; OG = organic-rich granitic.

Table 2
Click here to download Table: Table_2.docx

Table 2. Physical characteristics of the terrace soils.

Locality/ profile	Horizon	Depth (cm)	Gravel w.-%	Gravel vol.-%	Particle Size Distribution Sand (2-0.5 mm)	Silt (500-2µ)	Clay (<2µ)	Bulk density (g/cm^3)
Little Popo Agie - Red Canyon								
RCT2	A	0-9	0.6	0.3	27.2	49.2	23.6	1.2
	Bw1	9-21	0.9	0.5	22.1	51.3	26.6	1.4
	Bw2k	21-40	0.1	0.1	25.0	49.1	25.9	1.5
	CBk	40-60	0.2	0.2	26.4	49.5	24.2	1.7
	CK	60-90+	1.0	0.7	25.9	63.2	10.9	1.8
RCT3	A	0-7	14.2	7.0	39.1	44.9	16.1	1.2
	AB	7-30	13.2	7.4	37.3	42.2	20.5	1.4
	Bk1	30-50	22.3	14.0	38.5	44.2	17.3	1.5
	Bk2	50-100	32.1	23.3	60.6	34.7	4.7	1.7
	2C	100+	25.8	19.1	55.0	36.0	8.0	1.8
RCT4	A	0-10	23.3	12.1	35.5	46.1	18.5	1.2
	Bw1	10-18	14.7	8.4	40.9	41.6	17.5	1.4
	Bw2	18-30	34.2	22.8	27.0	49.4	23.6	1.5
	Bk1	30-50	33.9	21.3	22.5	47.0	30.5	1.4
	Bk2	50-100	14.6	9.4	27.2	41.7	31.1	1.6
	Ck	100-125	54.3	44.7	48.1	44.2	7.8	1.8
	C	125+	49.4	39.8	55.4	36.2	8.4	1.8
RCT5	A	0-15	6.6	3.1	32.4	47.1	20.4	1.2
	AB	15-25	30.6	17.8	52.1	30.5	17.4	1.3
	Bk	25-40	68.4	56.6	11.0	88.3	0.8	1.6
	Bkm	40-80	87.7	81.1	--	--	--	1.6
	Ck	80-200	55.4	45.8	90.3	7.4	2.2	1.8
Middle PopoAgie								

- Lander								
LWS-13-1	A	0-13	12.8	6.2	35.8	30.0	34.2	1.2
	Bt1	13-23	3.8	2.2	27.6	33.4	39.0	1.5
	Bt2	23-32	10.4	6.2	47.1	24.4	28.5	1.5
	Bk	32-120	37.0	28.5	71.9	25.0	3.0	1.8
	BCk	120-150	27.2	18.4	62.4	20.8	16.8	1.6
	C	150+	36.4	28.0	55.4	36.2	8.4	1.8
SB	A	0-10	14.9	7.3	59.9	27.4	12.8	1.2
	Bt	10-25	6.3	3.7	47.2	28.1	24.7	1.5
	Bk1	25-60	23.0	13.6	63.2	21.8	15.0	1.4
	Bk2	60-100	20.9	12.2	71.3	26.6	2.1	1.4
	C	100+	36.4	28.0	55.4	36.2	8.4	1.8
North Fork PopoAgie								
PB-13-1	A	0-5	8.6	4.1	70.0	23.4	6.6	1.2
	AB	5-18	10.3	5.3	69.3	23.6	7.1	1.3
	B	18-50	15.7	9.6	70.7	19.9	9.4	1.5
	BC	50+	15.9	9.7	74.1	16.9	9.0	1.5
GalPD	A	0-25	1.0	0.4	31.8	58.1	10.1	1.0
	Bw	25-45	0.4	0.2	31.5	58.8	9.7	1.1
	BC	45-70	2.7	1.2	24.9	51.6	23.5	1.2
	C1	70-90		0.0	55.2	30.3	14.5	1.2
	C2	90-120						
	C3	120+						
GR-13-1	Ak	0-10	25.7	11.5	70.7	24.9	4.4	1.0
	Btk	10-21	42.9	25.4	68.7	22.7	8.5	1.2
	Bk	21-52	43.5	31.7	72.2	20.4	7.3	1.6
	BCk	52-75	53.1	37.4	89.5	8.1	2.4	1.4
	Ck	75+	37.8	25.6	85.9	9.2	5.0	1.5
GR-13-2	A	0-5	8.5	3.4	66.4	25.1	8.5	1.0

	Bt1	5-18	12.3	8.7	56.5	20.3	23.2	1.8
	Bt2	18-30	13.9	9.8	57.5	19.7	22.9	1.8
	Bk	30-70	41.2	27.0	73.7	20.1	6.3	1.4
	C2	70-90	38.6	13.1	92.9	5.0	2.1	0.6
	C3	90+	36.4	12.1	94.6	3.2	2.2	0.6
PB-13-2	A	0-5	9.7	3.2	68.8	24.9	6.3	0.8
	Bt1	5-13	14.4	7.1	65.6	26.4	7.9	1.2
	Bt2	13-20	15.4	9.3	69.1	25.4	5.4	1.5
	Bt3k	20-30	22.5	16.5	59.8	23.1	17.1	1.8
	Bk1	30-50	43.8	37.0	76.1	15.2	8.7	2.0
	Bk2	50-90	40.3	33.8	71.5	18.1	10.4	2.0
	BCk / CBk	90+	27.9	19.0	84.7	13.0	2.3	1.6

Table 3
Click here to download Table: Table_3.docx

Table 3. Typical chemical characteristics of the terrace soils.

Locality	Horizon	Depth cm	pH ($CaCl_2$)	inorg. C g/kg	org. C g/kg	org. N g/kg	Org. C/N	Fe (ox)[1)] mg/kg	Al (ox)[1)] mg/kg	Mn (ox)[1)] mg/kg
Little PopoAgie - Red Canyon										
RCT2	A	0-9	7.31	5.0	35.7	9.26	3.9	350	647	158
	Bw1	9-21	7.44	5.7	11.2	7.43	1.5	367	726	168
	Bw2k	21-40	7.39	5.9	9.2	6.24	1.5	327	689	172
	CBk	40-60	7.58	10.6	8.9	6.15	1.4	305	666	214
	CK	60-90+	7.68	21.3	4.0	5.93	0.7	316	612	158
RCT3	A	0-7	7.52	6.3	18.5	6.62	2.8	223	589	323
	AB	7-30	7.58	10.9	13.2	6.32	2.1	182	529	264
	Bk1	30-50	7.67	50.9	7.8	6.08	1.3	24	116	58
	Bk2	50-100	7.92	49.0	2.8	4.57	0.6	76	207	92
	2C	100+	7.93	35.3	0.3	4.70	0.1	270	10	186
RCT4	A	0-10	7.39	10.1	19.5	5.32	3.7	375	1026	284
	Bw1	10-18	7.53	18.6	14.5	4.97	2.9	227	774	174
	Bw2	18-30	7.58	32.9	10.6	5.12	2.1	99	650	93
	Bk1	30-50	7.62	53.2	7.3	4.32	1.7	53	451	59
	Bk2	50-100	7.78	65.3	3.2	3.84	0.8	11	150	42
	Ck	100-125	8.03	48.3	2.7	3.68	0.7	120	283	105
	C	125+	7.80	22.0	0.6	3.58	0.2	70	43	265
RCT5	A	0-15	7.64	23.4	11.2	4.84	2.3	202	534	223
	AB	15-25	7.57	39.3	16.2	4.49	3.6	123	336	107
	Bk	25-40	7.73	62.6	8.1	3.92	2.1	45	104	35
	Bkm	40-80	7.91	81.7	2.7	3.09	0.9	19	10	48
	Ck	80-~200	7.99	43.8	2.3	2.54	0.9	91	130	132
Middle										

PopoAgie - Lander										
LWS-13-1	A	0-13	7.70	14.9	17.5	4.67	3.7	523	440	179
	Bt1	13-23	7.69	11.1	7.3	4.42	1.7	413	438	214
	Bt2	23-32	7.71	11.5	7.1	3.82	1.8	172	665	134
	Bk	32-120	7.70	40.5	1.9	3.28	0.6	10	72	37
	BCk	120-150	7.89	22.4	0.8	3.14	0.3	52	91	127
	C	150+								
SB	A	0-10	7.37	0.7	10.8	3.66	2.9	285	347	206
	Bt	10-25	7.49	0.9	5.8	3.80	1.5	364	491	234
	Bk1	25-60	7.69	63.3	5.0	4.01	1.2	47	131	20
	Bk2	60-100	7.88	53.0	1.8	4.57	0.4	79	78	37
	C	100+								
North Fork PopoAgie										
PB-13-1	A	0-5	6.40	0.6	20.6	2.82	7.3	1120	353	193
	AB	5-18	6.15	0.4	12.3	1.91	6.4	2267	335	260
	B	18-50	6.80	0.1	7.1	1.02	7.0	770	418	190
	BC	50+	7.05	2.5	6.2	1.65	3.8	2557	435	185
GalPD	A	0-25	7.50	8.3	20.4	6.01	3.4	400	558	155
	Bw	25-45	7.60	17.5	16.0	5.47	2.9	392	623	188
	BC	45-70	7.70	22.1	7.1	5.02	1.4	218	236	211
	C	70-90+	7.78	16.1	3.1	4.45	0.7	83	331	163
		90-120	7.83	15.4	1.5	3.47	0.4	10	241	337
		>120	7.80	12.9	1.5	3.96	0.4	10	164	506
GR-13-1	Ak	0-10	7.30	0.4	16.3	5.26	3.1	591	805	273
	Btk	10-21	7.35	0.1	15.5	4.75	3.3	258	1073	219
	Bk	21-52	7.60	28.1	8.2	3.83	2.1	165	434	111
	BCk	52-75	7.50	18.6	2.3	2.19	1.0	166	100	80
	Ck	75+	7.30	15.3	4.1	2.51	1.6	168	100	73

GR-13-2	A	0-5	6.18	0.0	10.1	3.57	2.8	385	287	149
	Bt1	5-18	6.53	1.4	6.7	3.74	1.8	271	893	100
	Bt2	18-30	6.80	2.3	5.9	3.77	1.6	130	1073	45
	Bk	30-70	7.54	29.5	9.9	3.95	2.5	48	669	3
	C2	70-90	7.74	54.4	5.2	3.93	1.3	107	33	7
	C3	90+	7.72	6.5	1.1	3.12	0.3	581	116	29
PB-13-2	A	0-5	7.50	1.4	21.7	4.46	4.9	350	505	251
	Bt1	5-13	7.30	1.0	14.4	3.09	4.7	291	514	229
	Bt2	13-20	7.50	7.0	14.3	2.38	6.0	180	568	162
	Bt3k	20-30	7.65	19.8	14.8	3.15	4.7	138	412	96
	Bk1	30-50	7.60	58.1	12.4	2.82	4.4	25	46	26
	Bk2	50-90	7.20	56.4	5.4	2.35	2.3	24	40	12
	BCk / CBk	90+	7.65	22.6	2.6	1.75	1.5	114	40	46

[1)]ox = oxalate-extractable fraction

Table 4
Click here to download Table: Table_4.docx

Table 4. Overview of the main soil minerals (obtained from XRD and DRIFT measurements) in the fraction < 32 µm (clay + fine silt)

Site (age)	Horizon	Quartz	Orthoclase	Albite	Mica	Vermiculite	Chlorite	Calcite	Dolomite	Kaolinite	Hematite
PB-13-1 (Holocene)	A	xxx	xx	xx	x				?	x	?
	AB	xxx	x	x	x	x	?	?	?	x	?
GR-13-1 (160 ky)	Ak	xxx	x	x	x	x		xx	x	x	(x)
	Btk	xxx	x	x	x	x		xx	x	x	(x)
	Bk	xxx	x	x	x	x		xx	?		
	Ck	xx	x	x	x	?		xxx	xx	x	?
PB-13-2 (660 ky)	A	xxx	xx	xx	x	x		x	?	x	(x)
	Bt1	xxx	xx	xx	xx	x		xx	?	x	(x)
	Bt2	xxx	x	xx	x	x		xxx	x	x	(x)
	Bt3k	xxx	x	x	x	?		xxx	?	x	(x)
	Bk1	xx	x	x	x	?		xxx	x	x	?
	BCk/CBk	xx	x	x	?	x		xxx	xx	(x)	(x)

Concentration indications
? questionable
(x) traces
x low amount
xx moderate amount
xxx high amount

Table 5
Click here to download Table: Table_5.docx

Table 5. Stocks and interval-accumulation rates for pedogenic $CaCO_3$.

Terrace age	$CaCO_3$ stocks kg/m^2	Average accumulation rates (linear trend) $g/m^2/y$	Time range (for accumulation rate)	Interval-Accumulation rates $g/m^2/y$
20 ky	16	0.79	0 - 20 ky	0.79
160 ky	314	1.96	20 - 160 ky	2.13
260 ky	393	1.51	160 - 260 ky	0.79
660 ky	469	0.71	260 - 660 ky	0.19

Appendix A

Click here to download Background dataset for online publication only: Appendix_1.docx